Palaeogeography, Palaeoclimatology, Palaeoecology 269 (2008) 189–204

Contents lists available at ScienceDirect

Palaeogeography, Palaeoclimatology, Palaeoecology

journal homepage: www.elsevier.com/locate/palaeo

Carbon isotope lateral variability in a Middle Frasnian carbonate platform (Belgium): Significance of facies, diagenesis and sea-level history

Anne-Christine da Silva *, Frédéric Boulvain

Pétrologie sédimentaire, B20, Université de Liège, Sart Tilman, 4000 Liège, Belgium

ARTICLE INFO

Article history:
Received 13 December 2005
Accepted 22 April 2008

Keywords:
Carbon and oxygen isotopes
Stratigraphy
Sequence architecture
Paleosol
Frasnian
Carbonate platform

ABSTRACT

Carbon isotopic variations of Frasnian shallow-water carbonates from Belgium are related to facies and major sea-level trends. The influence of the diagenetic overprint was assessed in order to determine the primary signal of the Frasnian carbonates. Shallow-water microfacies are characterized by biostromes with stromatoporoids and lagoonal deposits dominated by carbonate mud and calcareous algae with subaerial exposure surfaces. The diagenetic history was controlled by three main events: early meteoric diagenesis (short-term subaerial exposure during deposition), late meteoric diagenesis (major Famennian regression) and burial diagenesis. The oxygen isotopic values are almost constant with respect to facies, original material (carbonate mud and cement) and sedimentological units (no differences before or after the main regression). This homogeneity is related to resetting during late meteoric diagenesis. The carbon isotopic values are related to facies (with the more negative values for the shallowest facies) and to major sea-level variations (most negative values after the main regression). This pattern is interpreted as being related to primary signals. This trend was enhanced by early meteoric diagenesis and the influence of more negative values from paleosols. The carbon isotope patterns reflect the influence of sea-level and water circulation on shallow-water deposits and this influence implies that shallow-water carbonates are not necessarily good material for assessing the primary isotopic values of the ocean because of the influence of long residence time ("aging") of the platform-top water and because of early diagenesis.

1. Introduction

The Middle Frasnian (early Late Devonian) was a time of a globally warm (greenhouse) climate (for a recent review see Streel et al., 2000; Joachimski et al., 2004; Hladil et al., 2005) and of high sea level (Vail et al., 1977; Johnson et al., 1985; and for a recent review see Hladil, 2002). The combination of these environmental conditions allowed the development of vast epeiric seas with extensive shallow-water carbonates (Copper, 2002). Reef development was extremely intense (Kiessling et al., 1999) and the main reef-builders were stromatoporoids, tabulate and rugose corals, calcareous algae and cyanobacteria (for a review of Frasnian reefal systems, see Burchette, 1981; Wood, 1998; Kiessling et al., 1999; Copper, 2002). The Frasnian–Famennian (F–F, Mid–Late Devonian) boundary represents one of the five major extinction events in the Phanerozoic, with the extinction of 60 to 85% of the reef-building taxa (Copper, 2002).

Stable isotopic measurements have been carried out intensively on the F–F boundary strata by many authors in order to understand this critical period (Joachimski, 1997; Joachimski et al., 2001, 2002; Chen et al., 2002, 2005; Stephens and Sumner, 2003; Goddéris and Joachimski, 2004). House (2002) stressed that there were several extinction events during the Frasnian and that, in order to place the mass extinction in its Devonian context, it is especially important to study the entire Frasnian and not to focus only on the F–F boundary. Furthermore, other authors have identified an important positive carbon isotope excursion during the early Middle Frasnian *punctata* conodont zone (*punctata* Isotopic Event; Racki et al., 2004; Pisarzowska et al., 2006; Yans et al., 2007), demonstrating the importance of the overall Frasnian interval (Baliński et al., 2006). Carbon and oxygen isotope curves from the Middle Frasnian (following the formally approved stage subdivision by the Subcommission on Devonian Stratigraphy, SDS; Becker and House, 1998; SDS Business Meeting, Leicester, July 2006) carbonate platform in Belgium are presented here and placed in a global sedimentological context. The high quality Tailfer section was chosen for detailed sampling and analysis, and complementary data from three other lateral time-equivalent outcrops were also obtained. A preliminary study of the carbon isotope curve from the Tailfer section compared with magnetic susceptibility was previously presented in da Silva and Boulvain (2002).

The main objective of this paper is to propose a stable isotope transect from basinal to shallow-water platform settings. This will allow analysis of the impact of the environmental variations on shallow epeiric seawater geochemistry during the Frasnian, as well as the impact of early and late diagenesis on the geochemical evolution of the carbonate sediments.

* Corresponding author. Tel.: +32 4 3662258; fax: +32 4 3662921.
E-mail address: ac.dasilva@ulg.ac.be (A.-C. da Silva).

0031-0182/$ – see front matter © 2008 Elsevier B.V. All rights reserved.
doi:10.1016/j.palaeo.2008.04.029

2. Geological setting

The Frasnian limestones studied here belong to the Rhenohercynian fold and thrust belt (Fig. 1). During the Middle Frasnian, an extended carbonate platform developed in Belgium (da Silva and Boulvain, 2004). In the more distal part of the platform (in southwestern Belgium, southern border of the Dinant Synclinorium), a succession of three carbonate mound levels separated by shales is present (Moulin Liénaux and Grand Breux Formations) (Boulvain, 2001). In the intermediate part of the basin (Philippeville Anticline), argillaceous, crinoidal and biostromal facies (Pont-de-la-Folle and Philippeville Formations) developed and in the proximal part of the basin (northern border of the Dinant Synclinorium, Vesdre Synclinorium and southern border of the Namur Synclinorium), stromatoporoid biostromes and lagoonal facies appeared (Lustin Formation) (Fig. 1B). The Upper Frasnian contains more argillaceous formations. In the southern part of the basin, carbonate mounds (Petit Mont Member) are included in shales and nodular argillaceous limestone of the Neuville and Valisettes Formations. The northern part of the basin corresponds to the shale-dominated Aisemont and Lambermont Formations. The Middle Frasnian rocks studied here are dated from the *punctata* to Early *rhenana* Zones (Bultynck et al., 2000; Gouwy and Bultynck, 2000). Correlations between the studied sections based on sedimentological evolution and magnetic susceptibility are proposed in da Silva and Boulvain (2006).

Data come from the Villers, Tailfer, Barse, Aywaille and Colonster sections (Fig. 1). The Villers section is the most distal outcrop and is located in the Philippeville Anticlinorium. It belongs to the Philippeville Formation; all other sections belong to the Lustin Formation. The Tailfer and Barse sections are in the northern part of the Dinant Synclinorium and the Aywaille section is in the eastern part of the Dinant Synclinorium. The Colonster section is the most proximal one and belongs to the Vesdre Synclinorium.

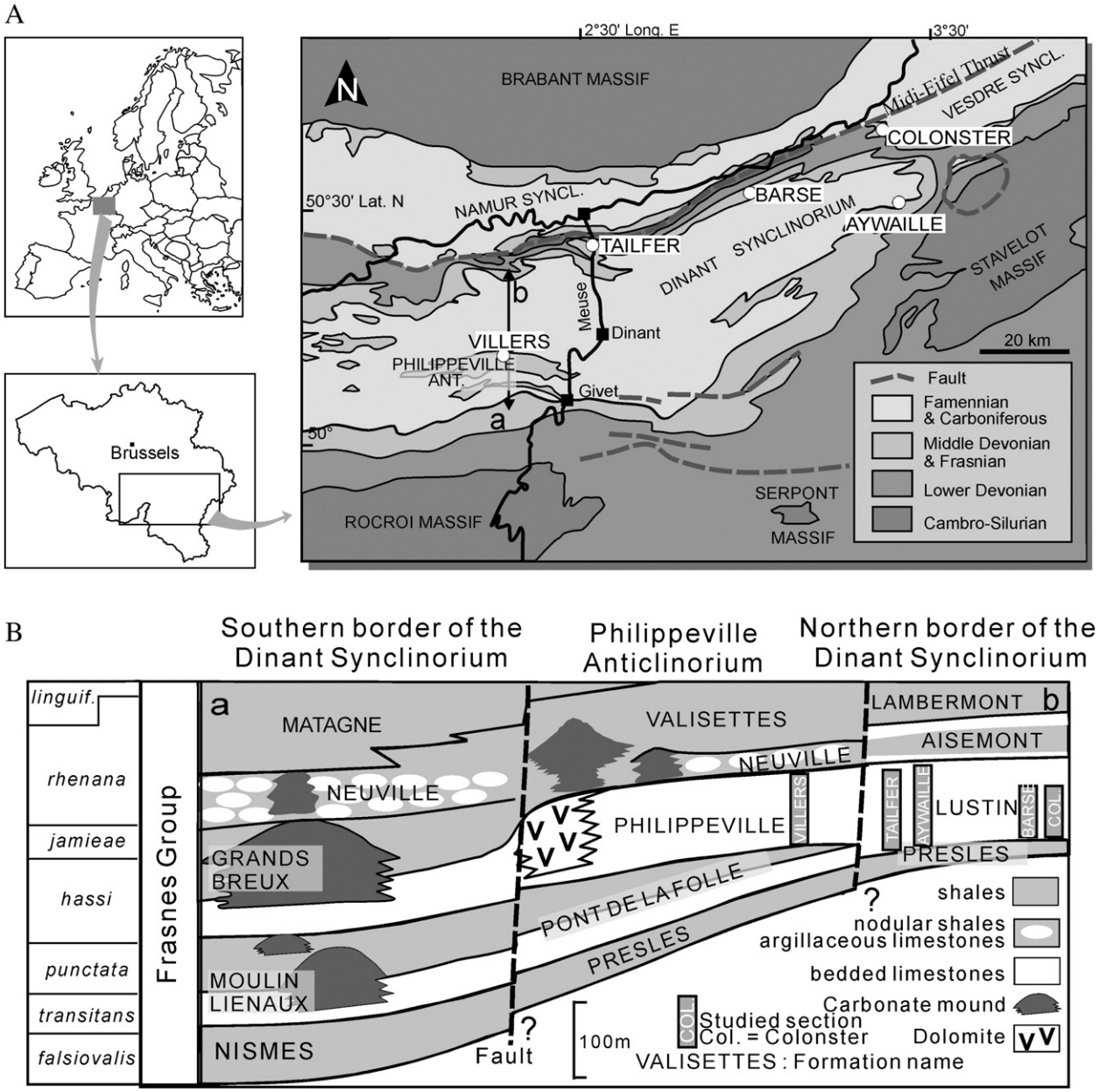

Fig. 1. A. geological map of Belgium, with location of the studied sections; B. North–south cross-section through the Belgian Frasnian sedimentary basin, before Variscan deformation. Letters a and b correspond to the cross-section line a–b on A.

In this paper, the Tailfer section is used as a reference to describe the sedimentological and isotopic evolution. This section has been chosen because it is the stratotype of the Lustin Formation (Boulvain et al., 1999); it covers a large part of the Frasnian without significant hiatus; it is not strongly affected by diagenesis; and it is exposed in an outstanding quarry with sawn rock faces, which allows very detailed observations. Concerning the other sections, two samples were analysed for each sedimentological unit (see Section 4.2). In addition to the sampling of carbonate mud, isotopic analyses were also performed on some brachiopods from the Aywaille, Barse and Colonster sections and on different cement generations (see Section 6.1) from the Tailfer, Barse and Villers sections.

3. Material and methods

3.1. Sedimentology

In the present study, the analysis of microfacies was based on the detailed study of more than 1000 thin thin-sections from five outcrops (Villers, Tailfer, Aywaille, Barse and Colonster). The maximum interval between two samples was 1 m. Classification of stromatoporoid morphology follows that proposed by Kershaw (1998). Facies and microfacies were compared with classic models (Wilson, 1975; Hardie, 1977; Flügel, 1982; James, 1983) and specifically with other Devonian platforms (May, 1992; Machel and Hunter, 1994; Méndez-Bedia et al., 1994; Pohler, 1998; Wood, 2000; Chen et al., 2001a; MacNeil and Jones, 2006).

3.2. Isotopic data

More than 140 analyses were performed on carbonate mudstone, including 130 analyses from the Tailfer section, five samples from the Aywaille section, four from Colonster and four from Villers. Samples consisted of the finest grained carbonate mudstone, without luminescence, with a minimal quantity of skeletal grains, clays and sparite from veins. In the shallow-water facies, brachiopods were almost absent; however, one non-luminescent brachiopod was found in the Colonster section, one in the Barse and another in the Aywaille section. Furthermore, eight analyses were performed on cement stages 2 and 4 (see Section 6.1 on the diagenetic history) in large cavities from the Tailfer, Barse and Villers sections. All the data are provided in Appendix A.

Samples were carefully extracted from polished slabs with a millimetre-diameter dental-drill, under a binocular microscope. All samples were investigated for evidence of diagenetic alteration under a cold cathode luminescence microscope (Technosyn Cold Cathodo-luminescence Model 8200 Mk3, operating at 15–20 kV and a vacuum of 0.2 to 0.01 Torr). The isotopic analyses were performed at the Institute of Geology and Mineralogy of the University of Erlangen, Germany. The carbonate powders were reacted with 100% phosphoric acid (density >1.9, Wachter and Hayes, 1985) at 75 °C in an online carbonate preparation line (Carbo-Kiel — single sample acid bath) connected to a Finnigan Mat 252 mass spectrometer. Results were reported in ‰ relative to V-PDB by assigning a $\delta^{13}C$ value of +1.95‰ and a $\delta^{18}O$ value of −2.20‰ to the NBS19 standard. Reproducibility was checked by replicate analysis of laboratory standards and was found to be better than ±0.1‰.

4. Sedimentological analyses

A detailed description of the carbonate platform is not the purpose of this paper; therefore, only a summary of the facies is provided. The complete sedimentological description of this platform is given by da Silva and Boulvain (2004). The facies are described from the more distal to the more proximal. The simplified sedimentological model is represented in Fig. 6D.

4.1. Facies, microfacies and paleoenvironments

4.1.1. External belt (microfacies 1–2)

This belt consists of decimetre-thick dark calcareous beds, with some argillaceous intercalations. Two microfacies are described, (1) wackestone rich in crinoids and sponge spicules (Plate IA) and (2) packstone or wackestone with crinoids and ostracods (Plate IB). Both microfacies are interpreted as being deposited below the fair-weather wave base (FWWB) but within storm weather wave base (SWWB); microfacies 2 is probably in a more proximal position.

4.1.2. Biostromal belt (microfacies 3–5):

The biostromes are mainly constructed by stromatoporoids with different morphologies: (3) laminar stromatoporoid biostromes (Plate IC), (4) rudstone with high domical stromatoporoids and rugose and tabulate corals (Plate ID) and (5) floatstone composed of dendroid stromatoporoid biostromes (Plate IE). These microfacies correspond to a biostromal belt, with low to strong wave energy, close to FWWB where the sediment was episodically reworked by storms.

4.1.3. Internal belt (microfacies 6–12):

The subtidal facies (6–8) are characterized by (6) floatstone with *Amphipora*, (7) packstone with paleosiphonocladales (Plate IF) and (8) packstone with peloids.

The intertidal facies (9–11) consist of (9) wackestone or packstone with *Umbella* (Plate IH), (10) carbonate mudstone with ostracods and (11) laminated grainstone with peloids (Plate IG).

The supratidal zone (12) is characterized by strongly brecciated decimetre- to metre-thick intervals (Plate II) cut by desiccation cracks. The clasts (centimetre- to decimetre-size) are generally elongated in the direction of stratification (Plate IIE); they are composed of the microfacies from the internal belt and are surrounded by microspar (Plate IIA to C). Circumgranular cracks (Plate IIA) are common and granular cement is often present within the cavities and under the clasts, forming brownish irregular pendants (Plate IIA and B). According to Wright (1994), all these features are characteristic of pedogenesis. Thus, this facies corresponds to the supratidal zone, with well-developed paleosol horizons.

4.2. Sedimentological evolution

Field observations on the Tailfer section and the stacking pattern of microfacies show that sediments are arranged into small, medium and large-scale sequences. This kind of stacking pattern is very common in Frasnian strata (McLean and Mountjoy, 1994; Brett and Baird, 1996; Elrick, 1996; Garland et al., 1996; Whalen et al., 2000; Chen et al., 2001b).

4.2.1. Small-scale sequences

The small-scale sequences correspond to a few beds (one to five beds, decimetre- to metre-thick) and show mainly a shallowing-upward trend. In this study, because the sampling interval was approximately 50 cm, the small-scale sequences were only identified in the field and not on the microfacies curve. For this reason, only the medium and large-scale sequences are considered in this paper.

4.2.2. Medium-scale sequences

The medium-scale sequences (see Tailfer section, Fig. 3b–c) are identified by the stacking of small-scale sequences; they are metre-thick and show both transgressive and regressive trends. They are mainly asymmetric, with a regressive tendency being usually dominant. These sequences are identified on the microfacies curve and in the field. These sequences can be correlated across the entire Lustin and Philippeville Formations, over a distance of more than 100 km.

During the approximately 0.4-My-long *jamieae* Zone (Kaufmann, 2006) two or three medium-scale sequences are observed and during the approximately 1.3-My-long *hassi* Zone (Kaufmann, 2006), four of these

sequences are recorded. Using these data, the medium-scale sequences have a calculated duration of 135 to 325 ky, which corresponds to a fourth-order sequence (Vail et al., 1977; Goldhammer et al., 1993).

This kind of fourth-order sequence is very common in carbonate platforms and different mechanisms have been suggested for their generation: (1) autocyclic tidal-flat progradation (Ginsburg, 1971; James, 1984); (2) episodic tectonic subsidence (Cloetingh, 1988); and (3) eustatic variations (Elrick and Read, 1991; Goldhammer et al., 1993). Eustatic variations are probably the most likely mechanism for explaining the generation of the sequences developed in the Frasnian carbonate platform of Belgium. In fact, the presence of transgressive bases below subtidal cycles in some sequences, the abundance of pedogenetic structures and the correlation of the sequences over 100 km are good arguments for a eustatic origin (Osleger, 1991; Elrick, 1995). Eustatic variations can be produced by glacio-eustasy during icehouses times, but the Frasnian is well known as a greenhouse period. In order to explain the development of eustatic sequences during greenhouse periods, some authors have proposed an influence of temperature changes and related ocean water volume changes, of cyclic evaporation of isolated oceanic basins (Donovan and Jones, 1979; Strasser, 1988) and of geoid deformation or variation in oceanic circulation (Mörner, 1994).

4.2.3. Large-scale sequences

The large-scale sequences are several tens of metres thick and their theoretical duration is greater than one million years, corresponding to third-order cycles (Vail et al., 1977; Goldhammer et al., 1993). The main sedimentological feature is an important facies shift from dominantly biostromal to lagoonal facies (Fig. 3). The first unit (first 50 m of the Lustin Formation in Tailfer) consists of biostromal and open-marine facies. This is called the "biostromal unit" and the constituent fourth-order sequences start with biostromal or open-marine deposits followed by lagoonal sediments (subtidal or intertidal). The second unit (upper 50 m of the Lustin Formation, Tailfer section) mainly consists of lagoonal deposits and is called the "lagoonal unit". The fourth-order sequences composing this lagoonal unit begin with lagoonal subtidal deposits followed by intertidal or supratidal sediments. The biostromal and lagoonal units are recognized all over the sedimentary depositional area (from the southern border of the Dinant Synclinorium to the northern border of the Namur Synclinorium), over distances of more than 200 km, and are probably related to sea-level variations.

Several charts of eustatic fluctuations during the Frasnian have been published (Johnson et al., 1985; Day, 1996; Whalen and Day, 2005; Bábek et al., 2007). Correlation with sea-level variations from another basin could make a good argument to support the idea of a eustatic origin for the third-order sequences discussed here. In the carbonate platforms of Western Alberta, Whalen and Day (2005) identified the position of an important sea-level change between the transgressive–regressive cycles IIc and IId in the *hassi* Zone. This transition could correspond to the boundary between the biostromal and lagoonal units. It can also correspond to the lower boundary of sequence #1 from MacNeil and Jones (2006). In Australia, Playford (2002, in Fig. 2, p.765) identified different sequences and the limit between his sequences 4 and 5 could also correspond to this boundary. Correlation of Devonian eustatic events worldwide is difficult considering that conodont zonal boundaries are not always very well constrained (see reviews in Sobstel et al., 2006; Zhuravlev et al., 2006). Thus, this coincidence of sea-level events between Alberta, Australia and Belgium could indicate a eustatic origin for the large-scale sequences recognized in this case study. However, the uncertainties in age dating do not permit unequivocal correlation or interpretation of a eustatic origin.

5. Diagenetic evolution

Diagenetic alteration of carbonates commonly obscures the primary carbon and oxygen isotopic signal. In order to determine whether the isotope signatures reflect the primary isotopic composition of seawater, the possible effects of diagenesis have to be assessed. In the deeper part of the external platform, in the southern border of the Dinant Synclinorium, isotopic data are available and a model of the diagenetic history of the Upper Frasnian carbonate mounds has been proposed (Boulvain et al., 1992; Boulvain, 1993, 2001). The diagenetic sequence has been found to be the following (see Boulvain, 2001, for a synthesis): (1) radiaxial calcite, (2) automorphic non-luminescent calcite, followed by (3) a bright orange luminescent fringe, (4) granular xenomorphic calcite with a dull orange luminescence, (5) iron-bearing saddle dolomite and (6) silicification.

The radiaxial cement (stage 1) does not show the oxygen isotope signature of marine Devonian cements but has the same signature as stages 2 and 3 ($\delta^{18}O$ between −7 and −9‰, mean value of −7.7‰) (Fig. 10). The radiaxial cement has thus been interpreted as a former HMC marine cement, which was isotopically and chemically reset during precipitation of the following stages (Boulvain, 2001). These stages (2 and 3) were related to a meteoric origin, in relation to an important regression during the Famennian (Boulvain, 2001). The last calcitic stage (stage 4) had strong negative oxygen isotope values ($\delta^{18}O$ between −9 and −12‰, mean value of −10.9‰) and is probably related to burial.

In the Lustin and Philippeville Formations (intermediate and shallower parts of the platform), the diagenetic record presents almost the same cement succession (da Silva, 2004) but distribution of these cements is different, mainly concerning the size of cavities. The Upper Frasnian carbonate mounds are characterized by a huge number of large cavities (more than 50 cm in length and that can affect more than 50% of the rock, Boulvain, 2001). on the other hand, in the Lustin Formation, cavities are uncommon and very small (<1 mm in diameter).

Considering the burial of the Frasnian strata and average geothermal gradient in Belgium (Helsen, 1995), the illite crystallinity and conodont colour alteration indices (Helsen, 1992; Fielitz and Mansy, 1999), the northern and southern part of the Dinant Synclinorium reached the range of temperature between 120° and 245 °C. The same succession of cements in the shallowest and in the deepest part of the platform leads to the suggestion that the diagenetic history was probably similar for the entire Frasnian platform.

6. Results

6.1. Carbon isotope data ($\delta^{13}C$)

The measurements on brachiopods furnished an average value of 2.2‰, with values of 2.8‰ from Aywaille, 2.0‰ from Barse and 1.9‰ from Colonster (see Appendix A).

The carbon isotope data obtained from the different cement stages of the Lustin and Philippeville Formations (see diagenetic history, Section 5) are consistent with brachiopod data. For stage 2 (automorphic non-luminescent calcite) the carbon isotope values range between 1.5 and 3.8‰ (mean value of 2.8‰) and for stage 4 (granular xenomorphic calcite with a dull orange luminescence), they are between 1.1 and 2.4‰ (mean value of 1.9‰).

Plate I. Illustration of the microfacies from the Frasnian carbonate platform from Belgium. A. Microfacies rich in crinoids and sponge spicules (microfacies 1), external belt. Villers outcrop, thin-section from sample V47d, normal light, Philippeville Formation. B. Packstone or wackestone with crinoids (microfacies 2), external belt. Villers outcrop, thin-section from sample V30, normal light, Philippeville Formation. C. Laminar stromatoporoid biostrome (microfacies 3), biostromal belt. Tailfer outcrop, field picture, bed number 53, Lustin Formation. Note that stratification is not horizontal and is indicated by S_0. D. Biostrome with bulbous stromatoporoids (microfacies 4), biostromal belt. Aywaille outcrop, field picture, bed number 71, Lustin Formation. E. Dendroid stromatoporoids biostrome (microfacies 5), biostromal belt. Tailfer outcrop, scanned thin-section L13, Lustin Formation. 1. Dendroid stromatoporoids (*Stachyodes*) and 2. Encrusting stromatoporoids. F. Packstone with paleosiphonocladales (microfacies 7), internal belt. Villers outcrop, thin-section from sample V123, normal light, Philippeville Formation. G. Laminated cryptalgal grainstone with peloids (microfacies 11), internal belt. Aywaille outcrop, thin-section from sample A153, normal light, Lustin Formation. H. Packstone with *Umbella* (microfacies 9), internal belt. Aywaille outcrop, thin-section from sample A107, normal light, Lustin Formation.

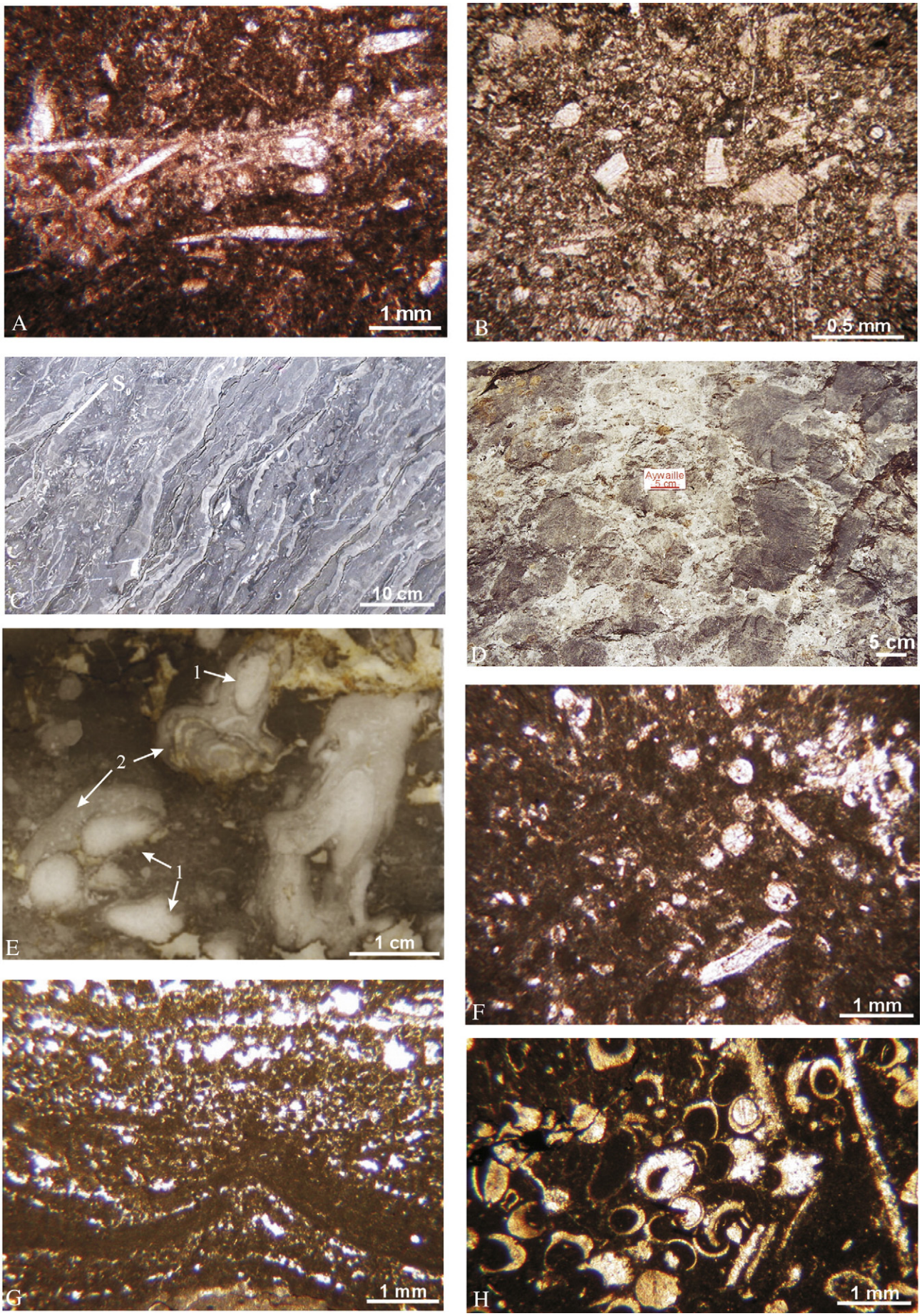
A
1 mm
B
0.5 mm
C
S0
10 cm
D
Aywaille
5 cm
5 cm
E
1
2
1
1 cm
F
1 mm
G
1 mm
H
1 mm

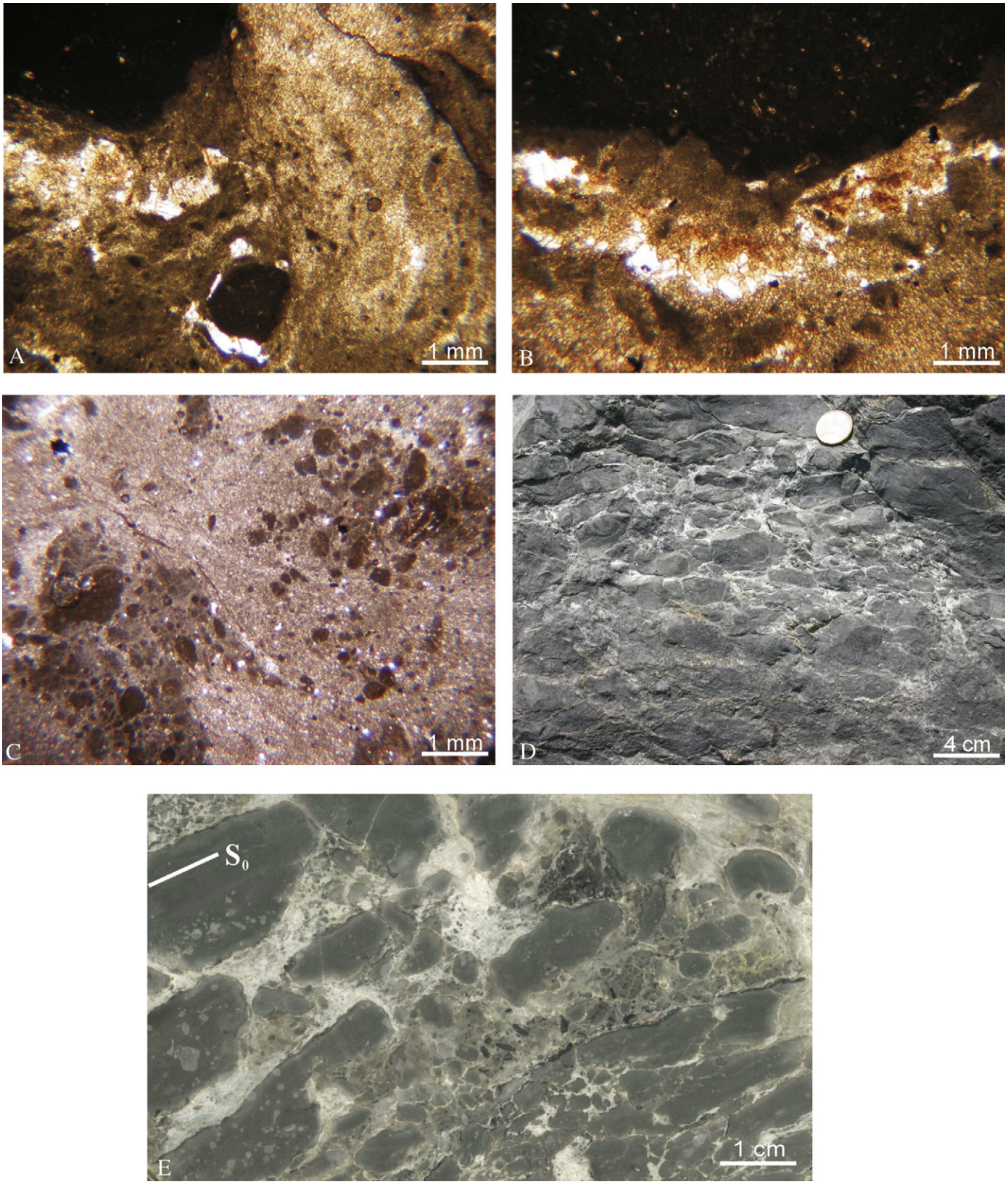

Plate II. Illustration of different pedogenetic structures, brecciated limestone, paleosol (microfacies 12), internal belt. A. Clasts in a microsparitic cement. The upper clasts show pendant cement and the smaller central clast is lined by circumgranular cracks. Tailfer outcrop, thin-section from sample L72c, normal light, Lustin Formation. B. Pendant cement under a clast. Tailfer outcrop, thin-section from sample L72c, normal light, Lustin Formation. C. Globules and clasts in a microsparitic cement. Tailfer outcrop, thin-section from sample L72, normal light, Lustin Formation. D. Brecciated limestone, Tailfer outcrop, field picture, bed number 72, Lustin Formation. E and D. Brecciated limestone, Tailfer outcrop, scanned polished sample, bed number 72, Lustin Formation. Note that stratification is not horizontal and is indicated by S_0.

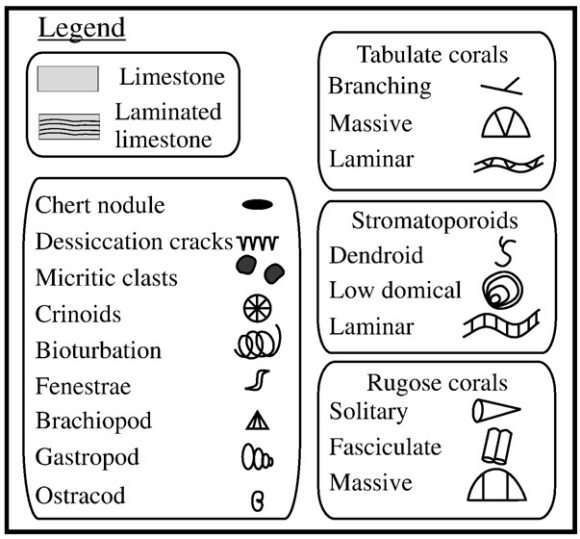

Fig. 2. Legend for lithological columns in Figs. 3 and 5.

For the Tailfer section, the carbon isotope values of matrix micrites are highly variable (mean values are given in Table 1). It is suggested that these variations are controlled by several factors:

(1) Sedimentological units (Figs. 3 and 4): in the biostromal unit, mean $\delta^{13}C$ values are around 3.0‰ and are relatively constant. In detail, in the Tailfer section, the first part of the biostromal unit shows more positive values (4.0‰ $\delta^{13}C$) compared to the second part (2.7‰ $\delta^{13}C$). The lagoonal unit has a more highly variable signature. Mean values are negative (−1.2‰ $\delta^{13}C$), with some values being strongly negative (−7.5‰ $\delta^{13}C$). The strong difference between the two sedimentological units is also evident in the Aywaille and Colonster sections (more negative carbon isotope ratios for the lagoonal unit) but this is not apparent in the Villers section, where $\delta^{13}C$ data are almost constant, around 2.4‰ (Fig. 4).

(2) Fourth-order sequences: when examined closely, the isotopic ratios from the lagoonal unit of the Tailfer section seem to be related to the fourth-order sequences (Fig. 3). For a majority of the regressive trends, carbon isotope values become more negative (from 0.0‰ $\delta^{13}C$ during the transgressive phase to −1.0 to −7.0‰ $\delta^{13}C$ for the regressive phase). This trend related to the fourth-order sequences is not obvious for the biostromal unit but appears for the regressive sequences of the lagoonal unit. In detail (Fig. 5), the tops of sequences 5 to 7 were subject to strong pedogenesis and, for these sequences, carbon isotope ratios reach highly negative values of −5.0 to −7.0‰. However, the tops of sequences 8 to 10 consist of intertidal facies and were not affected by pedogenesis; the isotope ratios remain between −1.0 and −3.0‰.

(3) Microfacies: the mean $\delta^{13}C$ values versus microfacies are shown for the Tailfer section (Fig. 6B). There is a clear trend towards more negative values of $\delta^{13}C$ from the deepest to the shallowest microfacies. For biostromal facies, ratios are from 3.0 to 1.6‰ $\delta^{13}C$. Subtidal microfacies (microfacies 6–8) have a mean value of 0.0‰ $\delta^{13}C$ (0.6 to −1.1‰ $\delta^{13}C$); intertidal facies (microfacies 9–11) have a mean value of −1.1‰ $\delta^{13}C$ (−0.8 to −2.0‰ $\delta^{13}C$); and supratidal facies (microfacies 12) show a mean value of −5.1‰ $\delta^{13}C$ (with a most negative value of −7.5‰). Fig. 6C shows the separated carbon isotope data for the biostromal and lagoonal units. For the biostromal unit, there is no clear relationship between facies and carbon isotope data. However, values from the lagoonal unit show an increasingly negative trend of carbon isotope ratio with facies evolving from the external to the internal zone and, finally, to the supratidal area.

(4) Subaerial exposure: the $\delta^{13}C$ data of the lagoonal unit are plotted versus the intensity of exposure (Fig. 7). In this paper, the intensity of exposure is subdivided in the following way:
  (1) Subtidal facies, not affected by pedogenesis; facies without any trace of exposure.
  (2) Intertidal facies, such as carbonate mudstone and laminar carbonate. These facies are periodically exposed and are characterized by stromatolites, pyrite, desiccation cracks and some evidence of reworking.
  (3) Supratidal facies with moderate pedogenesis, where the original microfacies are still recognizable: subtidal to intertidal facies, which were slightly transformed by pedogenesis (thin pedogenic horizons, less than 10 cm thick). The main observed features are the presence of pyrite, local microsparitization, desiccation cracks and first traces of brecciation.
  (4) Supratidal facies with strong pedogenesis, where the original microfacies is not always recognizable: subtidal to intertidal facies, which were strongly transformed by deeply penetrating pedogenesis (pedogenetic horizons one to several decimetres thick). The main observed characteristics are the presence of pyrite (and oxidized pyrite), intense microsparitization, illuviation, desiccation cracks, meniscus cements and intense brecciation (e.g. see Plate II). Carbon isotope signature becomes more negative in relation to increasing intensity of exposure (Fig. 7). Unexposed subtidal facies (0) have values of −0.6‰; intertidal facies (1), −1.1‰; supratidal facies with low pedogenesis (2), −2.1‰ and supratidal facies with strong pedogenesis (3) reach very negative isotopic values, such as −4.1‰.

(5) Position of the different sections in the basin: in Fig. 8, the mean values of $\delta^{13}C$ for each sedimentological unit are plotted for all sections, arranged from the most distal (Villers) to the most proximal (Colonster). Despite low sample density, the mean carbon isotope values of the lagoonal unit suggest an increasingly negative trend, from 2.0‰ in Villers to −4.4‰ in Colonster. However, mean $\delta^{13}C$ values of the biostromal units show a less negative trend, from 2.8‰ in Villers to 1.8‰ in Colonster.

6.2. Oxygen isotope data ($\delta^{18}O$)

The mean $\delta^{18}O$ values of brachiopods are similar, with brachiopods from the Aywaille section having a mean of −6.4‰, from the Barse section having a mean of −4.5‰ and from the Colonster section having a mean −7.1‰; their combined mean value is −6‰ (Appendix A).

Table 1
Carbon and oxygen isotopic mean, maximum and minimum values for the matrix of the Tailfer section and Frasnian carbonate mean values from the literature

	$\delta^{13}C$ (‰ PDB)	$\delta^{13}O$ (‰ PDB)
Biostromal unit (analysis of micrite)		
Mean values	3.0	−6.6
Minimum value	1.2	−5.0
Maximum value	4.8	−14.2
Lagoonal unit (analysis of micrite)		
Mean values	−1.2	−6.9
Minimum value	−1.75	−5.0
Maximum value	2.2	−13.9
Published marine carbonate Frasnian values		
Hurley and Lohmann (1989) Canning basin	1.5 to 2.5	−5.0 to −7.5
Viezer et al. (1986), Paleozoic brachiopods	−1.0 to 2.0	−5.5 to −7.5
Viezer et al. (1999), Paleozoic mean values	0.0 to 2.0	−4.5 to −7.5
Chen et al. (2002), South China		−6.0

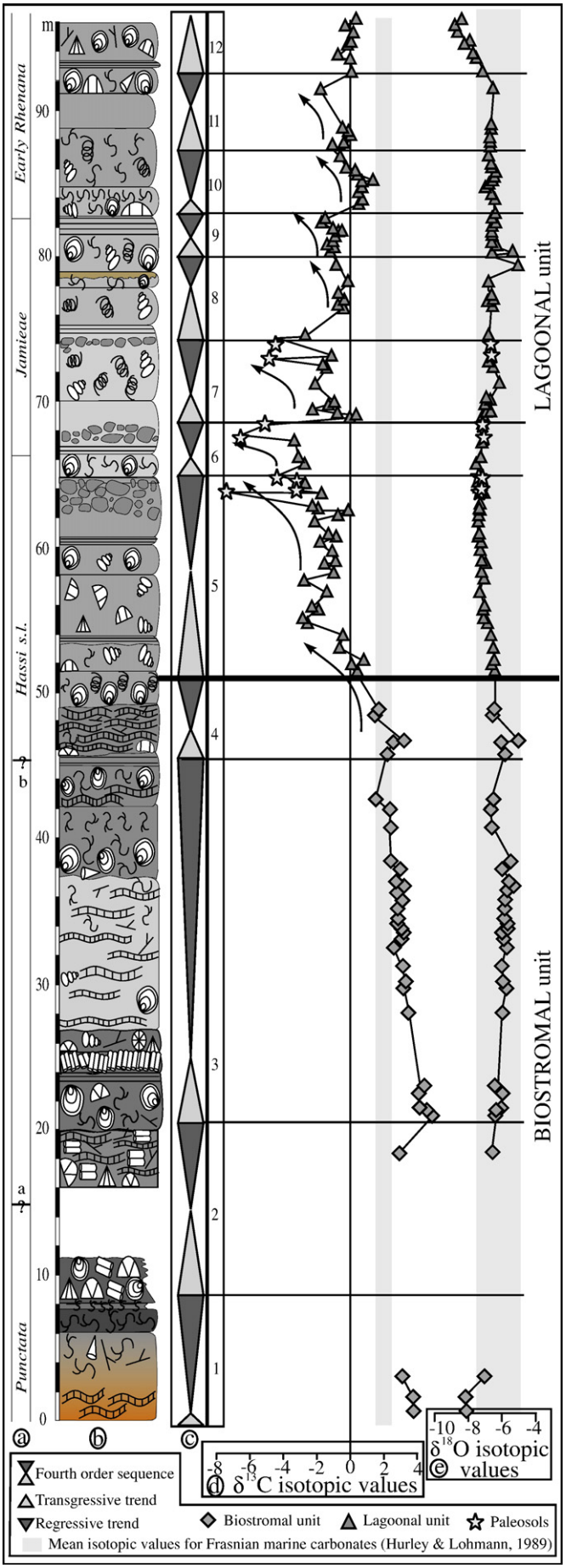

The oxygen isotope data obtained from the different cement stages of the Lustin and Philippeville Formations (see diagenetic history, Section 5) are more variable. For stage 2 (automorphic non-luminescent calcite), the oxygen isotope values range between −5.8 and −10.4‰ (mean value of −7.5‰) and for cement 4 (granular xenomorphic calcite with a dull orange luminescence), they are between −3.9 and −7.2‰ (mean value of −7.4‰) (Fig. 10).

For the Tailfer section, the oxygen isotope values of the matrix micrites are almost constant, with a mean $\delta^{18}O$ value of −6.6‰ (Table 1). There are no significant differences between the biostromal unit (−6.6‰ $\delta^{18}O$) and the lagoonal unit (−6.9‰ $\delta^{18}O$) (Table 1) or between the studied sections (Fig. 8). When compared with the microfacies (Fig. 6) and with the fourth-order sequences (Fig. 3), oxygen isotope values appear very homogeneous. Oxygen isotope values do not seem to be related to facies or to sedimentological units.

Considering the different carbonate materials analysed for the Lustin and Philippeville Formations, matrix, brachiopod shells and meteoric and burial cements show almost constant values, which fit within the same range, mainly between −6 and −7‰.

6.3. Patterns in $\delta^{13}C$ versus $\delta^{18}O$

Frasnian matrix micrites present a characteristic pattern, mainly based on highly variable carbon isotope and homogeneous oxygen data (Fig. 9). As noted, the main trends are constrained by the $\delta^{13}C$ values (with $\delta^{18}O$ almost constant). The first group (Fig. 9, Circles 1a and 1b) corresponds to the isotopic values of the biostromal unit showing the higher $\delta^{13}C$ values (3.0‰ $\delta^{13}C$). It can be divided into two parts, with the lower 30 m showing mean $\delta^{13}C$ values of around 4.0‰ (Circle 1a) and the upper 20 m of around 2.7‰ (Circle 1b). The second group (Circle 2, second trend) corresponds to the $\delta^{13}C$ values of the lagoonal unit and is largely negative, and the last group (Circle 3, third trend) corresponds to paleosols and is strongly negative.

7. Discussion and interpretation

In the light of the facies and diagenetic analyses, it is clear that different factors have affected the isotopic evolution following deposition. These are (1) early meteoric diagenesis during short-time subaerial exposure, corresponding to high-frequency, low-amplitude sea-level oscillations that exposed the platform, (2) late meteoric diagenesis, caused by a phreatic meteoric lens that invaded the Frasnian sediments during a major Famennian regression (Boulvain, 2001) and, finally, (3) burial diagenesis. The main diagenetic impact usually occurs during early diagenesis and generally leads to ^{18}O and ^{13}C depletion (Meyers and Lohmann, 1985; Banner and Hanson, 1990). After Veizer et al. (1999), once the rock is lithified, ^{18}O depletion is less pronounced, except during low-grade metamorphism.

7.1. Carbon isotope values ($\delta^{13}C$) and diagenetic alteration

Published carbon isotope values for Devonian marine carbonate are given in Table 1 (Veizer et al., 1986, 1999; Hurley and Lohmann, 1989; Chen et al., 2002) and vary between 0‰ and 2.5‰. For the Late *hassi* Zone to *rhenana* Zone interval studied here, Joachimski et al. (2002) obtained values of 0 to 2‰ from the Devils Gate section, Nevada.

Mean $\delta^{13}C$ values of the biostromal unit are around 3.0‰, which is higher than published marine carbonate data. Considering that diagenesis generally leads to isotope depletion, it seems that the carbon isotope values from the biostromal unit have probably not

Fig. 3. The Tailfer section. a. Conodont zonation after Gouwy and Bultynck (2000) (boundary 'a' between *punctata* and *hassi* Zones) and Bultynck et al. (2000) (boundary 'b' between *punctata* and *hassi* Zones). b. Lithological column (for legend, see Fig. 2); c. Fourth-order sequences, light grey pointing-up triangles are transgressive phases and dark grey pointing-down triangles are regressive phases; d. $\delta^{13}C$ isotopic values; e. $\delta^{18}O$ isotopic values.

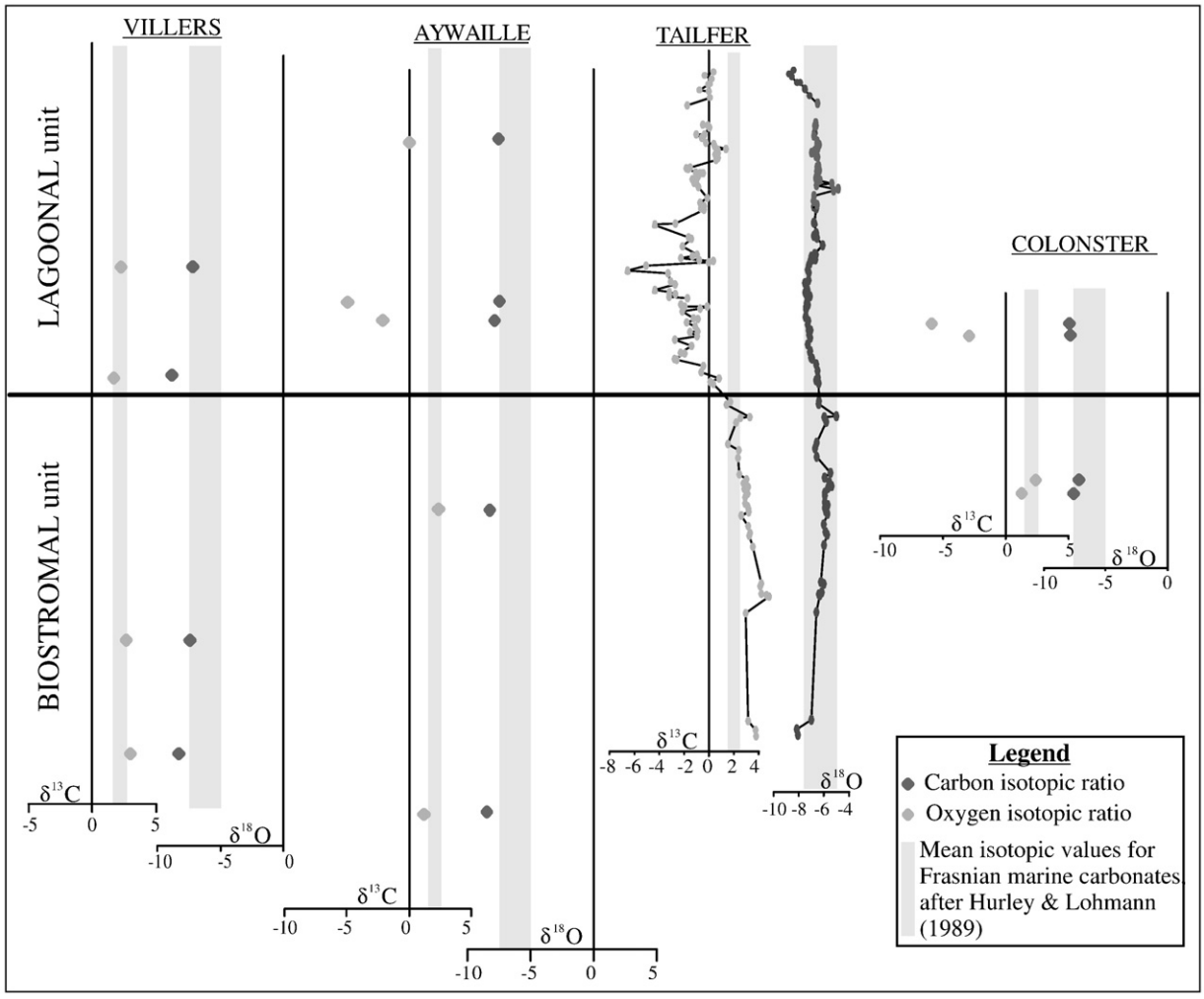

Fig. 4. Carbon and oxygen isotopic trends for the four studied sections [arranged from the most distal (Villers) to the most proximal (Colonster), see Fig. 1].

been affected by diagenesis. Discussion of these values is given below. By way of comparison, carbon isotope data from the lagoonal unit are depleted with respect to Devonian marine carbonate. It is therefore necessary to assess the influence of diagenesis for these facies.

7.1.1. Meteoric diagenesis

The carbon isotope data for the matrix micrites of the lagoonal unit (Fig. 9, Circle 2) are mainly negative and low (−1.2‰). The evolution towards more negative carbon isotopic values is observed to the top of fourth-order regressive sequences (as in Algeo et al., 1992), in transects from distal to proximal facies (as in recent sediments in Florida (Lloyd, 1964) and Barbados (Allan and Matthews, 1977, 1982) and in the Cretaceous of the Jura Mountains (Joachimski, 1994)), for the paleosols (Fig. 9, Circle 3, "third group" of values) and for the most proximal section (Colonster) (Fig. 8).

In this case, early meteoric diagenesis, exposure rate and pedogenesis are probably the most important processes affecting the carbon isotope ratios. Different authors have noted the association of exposure surface with pedogenesis and depleted ^{13}C signal (Allan and Matthews, 1977; Goldstein, 1991; Algeo et al., 1992; Joachimski, 1994; Algeo, 1996; Buonocunto et al., 2002, etc.). Furthermore, in the Belgian Frasnian carbonate platform, the biostromal unit and Villers section that are not affected by pedogenesis show normal marine isotope values.

The influence of pedogenesis on the isotope ratios is probably related to the pedogenesis rate and duration (Fig. 7). Joachimski (1994) and Algeo (1996) showed that carbon isotope trends can be correlated with increasing pedogenetic modifications in the sequences. This increasing pedogenesis increases porosity and permeability (desiccation cracks, roots, brecciation) and the water–rock ratio, and also allows enhanced fluid percolation. These fluids are charged in dissolved CO_2 derived from the oxidation of continental organic matter (Keith and Parker, 1965).

The biostromal and lagoonal units were both affected by late meteoric diagenesis (presence of meteoric cement in both units) but the biostromal unit was not affected by early meteoric diagenesis (no traces of subaerial exposure). The fact that isotopic data from the biostromal unit are not depleted in carbon supports the argument that, in our case, late meteoric diagenesis probably did not have a strong influence on the carbon isotopes.

7.1.2. Burial diagenesis

Significant burial alteration of carbon isotope signals requires a large water–rock ratio. However, in the Philippeville and Lustin Formations, the micrite samples are from massive carbonate rock, and the porosity of these carbonates is very low, with a high micritic content and a few small cavities. Furthermore, burial diagenetic alteration commonly leads to a reduction of $\delta^{13}C$ variations and homogenization of carbon isotopes (see for example Algeo et al., 1992). The carbon isotopes of matrix micrites from the Frasnian certainly do not reflect homogenization and so are probably not affected by burial.

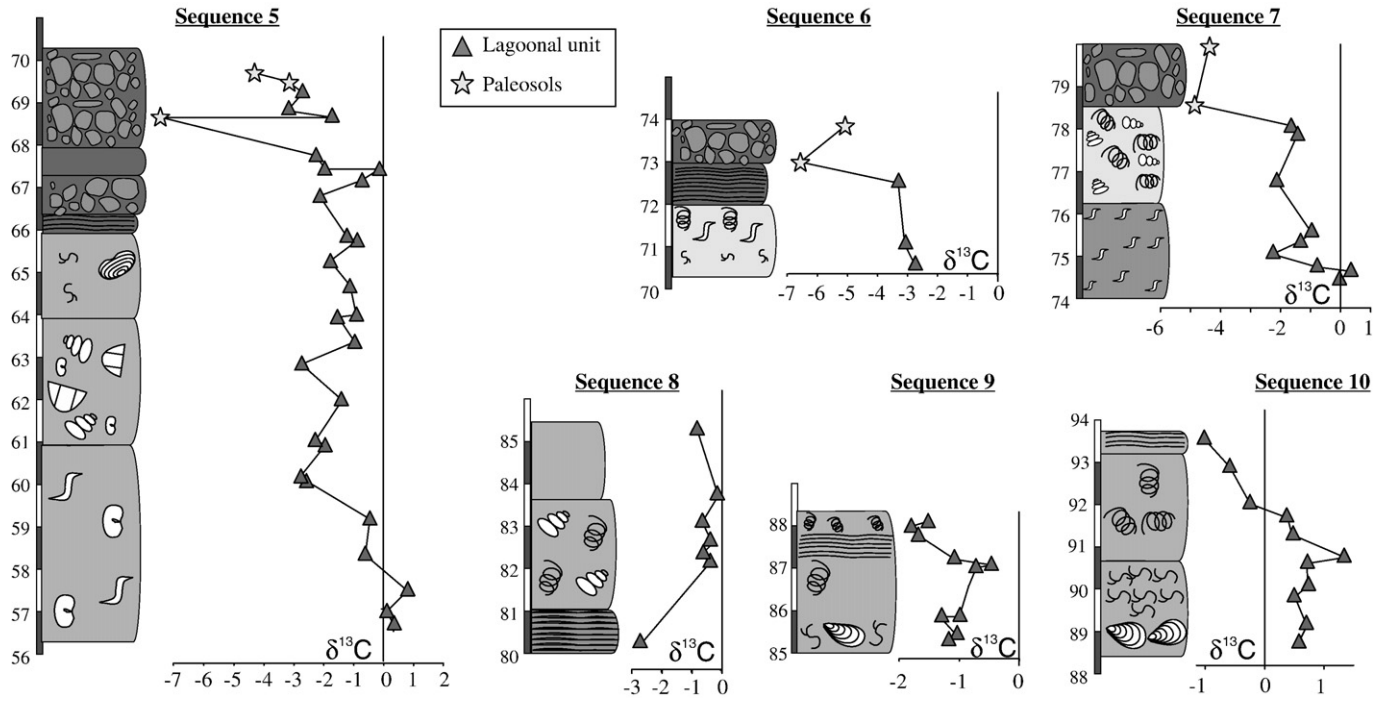

Fig. 5. Examples of fourth-order sequences from the Tailfer section (these sequences are represented on the complete lithological column of the Tailfer section on Fig. 3c), with carbon isotopic evolution. For legend, see Fig. 2.

7.2. Oxygen isotope data ($\delta^{18}O$) and diagenetic alteration

It was noted above that the oxygen isotope values of the micritic matrix and brachiopods are almost constant, around −7‰. In spite of the large number of oxygen isotope analyses of Devonian marine carbonate (Table 1) few studies have considered the middle part of the Frasnian. Joachimski et al. (2004) presented oxygen isotope data from biogenic calcite from different locations within the *jamieae* and *rhenana* Zones, which range between −4.6‰ and −6.8‰. The oxygen isotope data obtained from matrix micrites, brachiopods and cements are very homogeneous and correspond to the most negative values measured on some Devonian carbonates.

7.2.1. Meteoric diagenesis

The typical trend of an exposure surface is more negative $\delta^{13}C$ associated with more negative $\delta^{18}O$ due to the addition of lighter meteoric derived ^{16}O (e.g., Tucker and Wright, 1990; Buonocunto et al., 2002; Marquillas et al., 2007). But in this study, the oxygen isotope values are homogeneous and micrite $\delta^{18}O$ values of paleosols do not show negative shifts. The relative homogeneity of $\delta^{18}O$ and the high variability of $\delta^{13}C$ is a characteristic of a meteoric phreatic system ("meteoric water line" from Lohman, 1988). Allan and Matthews (1982) reported that homogeneous $\delta^{18}O$ values and very variable $\delta^{13}C$ values are common in shallow-water carbonates.

Allan and Matthews (1982) suggested that $\delta^{18}O$ tends to be homogeneous because meteoric water is a ubiquitous source of oxygen for the formation of new calcium carbonate during the process of cementation, recrystallization and replacement. The number of moles of oxygen derived from limestone compared to the number of moles of oxygen derived from water presents a very low ratio in a meteoric phreatic system. As a result of this, repeated dissolution–reprecipitation reactions will not noticeably change this ratio of the groundwater or of the diagenetically altered limestones and concomitantly precipitated cements. Therefore the $\delta^{18}O$ of limestones should remain relatively constant without important changes beneath subaerial exposure. Thus, it seems that in this Devonian case, early meteoric effects on oxygen isotopes were obliterated by resetting during a late meteoric diagenetic event.

7.2.2. Burial diagenesis

During burial diagenesis, the isotopic composition of the diagenetic phase is a function of the pore fluid and of the initial rock composition, water/rock ratio and temperature at the time of fluid rock equilibration. A high water/rock ratio (for example a rock with a larger open volume) yields to a diagenetic phase closer in isotopic composition to that of the pore fluid (greater ^{18}O depletion). Conversely, a low water/rock ratio yields to a diagenetic phase closer in composition to that of the host rock. In the carbonate mounds, the original porosity was very high, with many large cavities. This high porosity was not completely filled after the meteoric stage, considering the important volume of cement stage 4. In the mud mounds, the water/rock ratio was probably very high, resulting in a diagenetic phase strongly depleted in ^{18}O ($\delta^{18}O$ ratio of between −9 and −12‰; Fig. 10). This high water/rock ratio also led to recrystallization and isotopic depletion of the matrix micrites.

In the shallowest part of the platform (Lustin and Philippeville Formations), the majority of micrite samples are from massive carbonate rocks, without important open or filled porosity. Furthermore, the fact that original $\delta^{13}C$ values are retained argues for low water/rock ratios during burial diagenesis (Algeo et al., 1992). Finally, the fact that the oxygen isotope values are still homogeneous and not strongly depleted is also an argument for a small influence of burial on the isotopic composition, as opposed to the mud mounds, which exhibit a broader range and more depleted $\delta^{18}O$ values (Fig. 10).

7.3. Evolution of the carbon isotope composition of Frasnian seawater

The oxygen isotopes are completely homogenized by diagenesis and this diagenetic overprint obscures the primary signal of Frasnian seawater in our Belgian examples. The carbon isotope signatures were less affected by diagenetic processes and could give some clues to the primary seawater signal.

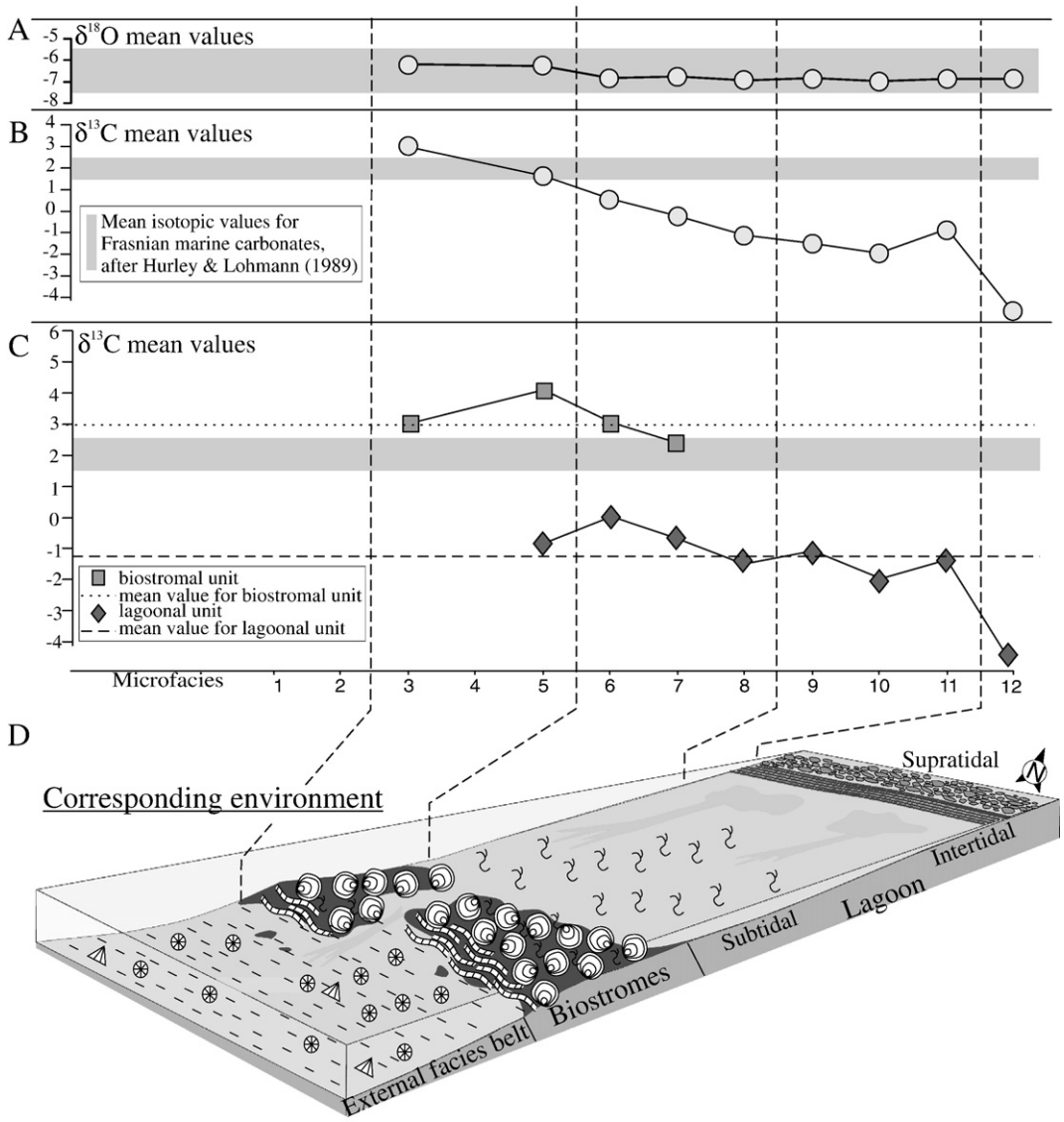

Fig. 6. Comparison of isotopic trends and environmental conditions. A. Mean oxygen isotopic values in the Tailfer section for each facies; B. Mean carbon isotopic values in the Tailfer section for each facies; C. Mean carbon isotopic values for the biostromal and the lagoonal unit for each facies; D. Simplified sedimentological model for the Frasnian of Belgium (after da Silva and Boulvain, 2004).

Carbon isotope records from epeiric-sea carbonates have been widely used as a proxy for secular changes in ocean chemistry. However, numerous authors have mentioned the difficulty of using carbon isotopes as a proxy for the global carbon cycle, noting the impact of local-scale variations in the carbon cycle in shallow-water seas. These can lead to lateral variations in carbon isotope values in carbonates and these variations may be preserved as a vertical trend (e.g., Holmden et al., 1998, 2006; Panchuk et al., 2005, 2006).

The signature of Frasnian seawater seems to have been different during deposition of the biostromal unit, compared to the lagoonal unit. Regarding the lagoonal unit, the low carbon isotope values could all be related to early meteoric diagenesis, or it could be that regionally the Frasnian seawater became depleted in ^{13}C in some areas of the platform. The second hypothesis seems more likely. The boundary between the biostromal and lagoonal units represents an important regression. This regression probably led to a restriction of the platform. This restriction is marked, for example, by microfacies 9, which only appears within the lagoonal unit. This facies is characterized by the abundance of the charophyte algea *Umbella* which, according to Mamet (1970), was significant in a littoral environment of extreme salinity.

In the case of modern semi-restricted marine environments, the influence of the local carbon cycle on $\delta^{13}C$ can be substantial. Effectively, the shallow water of Florida Bay and the Bahama Platform has a $\delta^{13}C$ value of 4.0‰ lower than the open-ocean surface water (Lloyd, 1964; Patterson and Walter, 1994). These low values have been linked to the input of ^{12}C from remineralized organic carbon during the long residence time ("aging") of the water on the platform (Patterson and Walter, 1994). This kind of lateral variation, with the lowest carbon isotope values in the shallowest part of the platform, has also been observed in Paleozoic sediments (see for example Holmden et al., 1998; Immenhauser et al., 2002). This was probably also the case during the deposition of the lagoonal unit. All the trends obtained here correspond to a proximal–distal gradient in $\delta^{13}C$ values, with the lowest values being in the shallowest zones (Figs. 5–8). Furthermore, subtidal lagoonal facies unaffected by pedogenesis are also depleted in ^{13}C ($\delta^{13}C$ of between 1.0‰ and −1‰). Sequences 8 to 12 are free of any traces of pedogenesis but are also depleted in ^{13}C. As noted earlier, the impact of late meteoric diagenesis on carbon isotope signatures was probably low, so this depletion, without a direct link to subaerial exposure, is probably related to original variations in seawater.

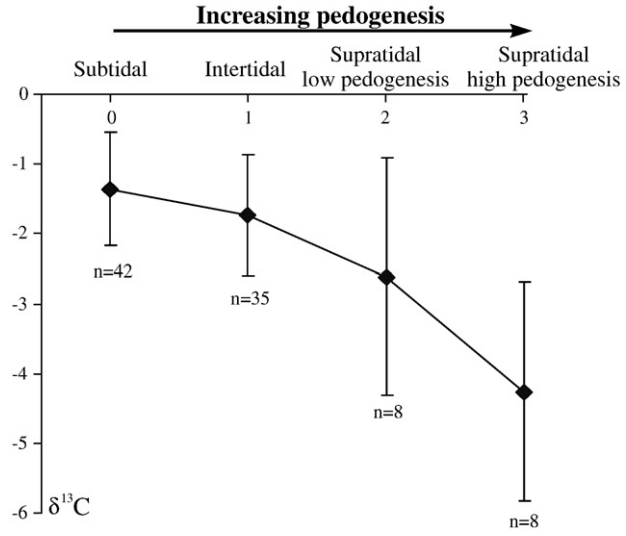

Fig. 7. Mean carbon and oxygen isotopic values for different degrees of pedogenesis for the lagoonal unit samples (for explanation of pedogenetic rate, see Section 6.1). *n* corresponds to the number of samples used to determine the average value.

During the deposition of the biostromal unit, it seems there was little lateral variation in the chemistry of Frasnian seawater. In fact, the values for the biostromal unit are almost homogeneous (around 3.0‰). There are no strong differences between the deepest facies and the lagoonal facies (mainly subtidal facies), neither of which are depleted in ^{13}C (Fig. 6C). Furthermore, in the biostromal unit, the carbon isotope values are abnormally positive, mainly for the lower part of this unit (Fig. 3, lower 30 m and Fig. 10, Circle 1a; mean values of around 4.0‰ with the highest value being 4.9‰). These values are higher than the carbon isotope values for Devonian marine carbonates (between 0 and 2.5‰); however, these high positive values are consistent with other measurements from the *punctata* Zone. Brachiopod carbon isotope data from the Arche Member in the southern Belgium (lateral time equivalent to the Tailfer section) range between 4 and 5‰ (Yans et al., 2007). These positive values have also been observed in Moravia (Hladikova et al., 1997; Gerls and Hladil, 2004) and in Poland (Racki et al., 2004; Pisarzowska et al., 2006). This convergence of data confirms the reliability of the measurements and the global nature of these high values. This is also an argument that, during this period, the sea was not restricted as it was during deposition of the

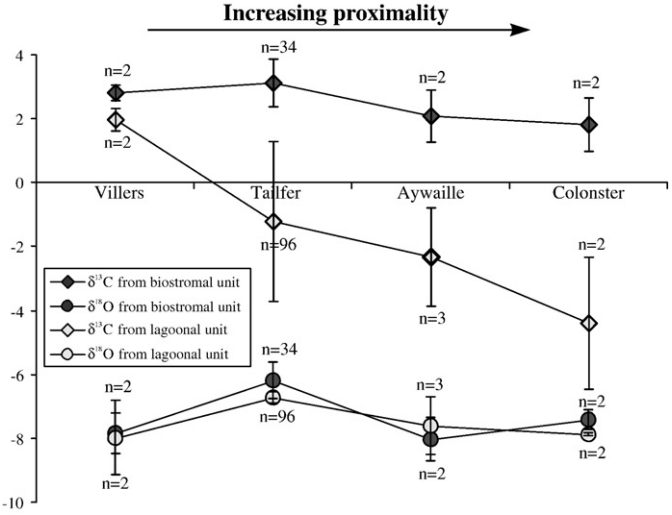

Fig. 8. Mean carbon and oxygen isotopic values for the sedimentological unit and for the studied sections arranged from the most distal to the most proximal localities (see Fig. 1). *n* corresponds to the number of samples used to determine the average value.

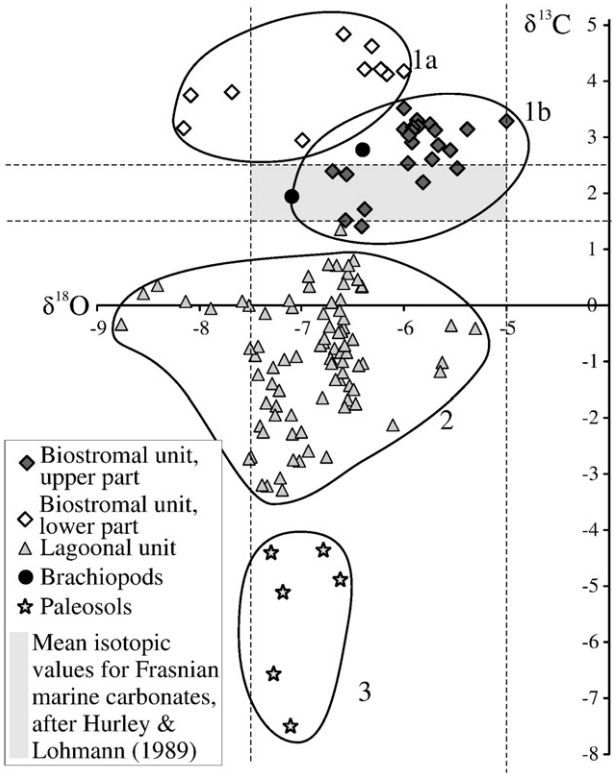

Fig. 9. Carbon and oxygen isotopic values for the Tailfer section, for the biostromal unit, lagoonal unit and paleosols.

lagoonal unit, so that its open-marine nature reduced or removed the lateral variability of the seawater carbon isotopic signature.

Other processes also affect the carbon isotopic ratio of seawater, such as oxidation of organic detritus in the water column, on the sea floor and in the sediment, weathering of carbonate and silicate rocks on land and changes in primary productivity and/or burial. According to Panchuk et al. (2006), the relative contribution of these processes to the $\delta^{13}C$ signal depends in part on water depth and structure and on

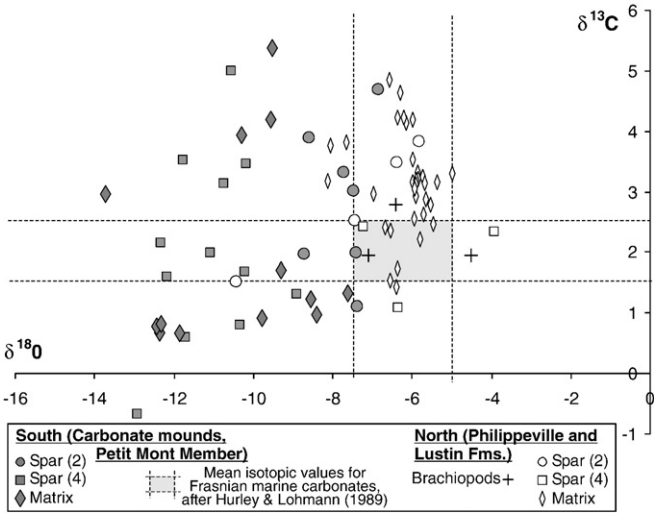

Fig. 10. Carbon and oxygen isotopic values for the different cement generations and for the matrix, from the carbonate mound Petit Mont Member, in the deeper part of the basin along the southern border of the Dinant Synclinorium (data from Boulvain, 2001), and from the Philippeville and the Lustin Formations (matrix values are from the biostromal unit).

rates and patterns of seawater circulation across the epeiric seas and between the epeiric seas and ocean.

In this Devonian case, sea level, water depth and structure and seawater circulation appear to have strongly influenced the carbon isotopic ratio of the Frasnian sea. In fact, during the deposition of the biostromal unit, sea level was relatively high and the Frasnian sea relatively open. An important regression at the beginning of the lagoonal unit probably changed the configuration of the Belgian Frasnian sea leading to restriction in the area of deposition of the Lustin Formation (this was probably not the case for the Philippeville Formation, which corresponds to another area where carbon isotopes were not depleted). This restriction is marked by new biotas such as *Umbella* and by more negative carbon isotopes through the long residence time ("aging") of platform-top shallow water (Patterson and Walter, 1994). The last few metres of the Lustin Formation, before the shaly biostromes of the Aisemont Formation, are characterized by a transgression, with the reappearance of open faunas such as crinoids and brachiopods. The carbon isotopes signatures increased with the transgression and, at the top of the Lustin Formation (Fig. 3), carbon isotope values are around zero, which corresponds probably to a reopening of the Belgian Frasnian sea and increasing water circulation. Actually, Immenhauser et al. (2003) proposed that, in epeiric seas, local effects are the rule, rather than the exception (see also discussion in Patterson and Walter, 1994; Holmden et al., 1998). These local effects will lead to low values for platform-top carbonates (as in our example), due to ^{13}C depleted soil effects and to "seawater aging". A rapid deepening will enhance water circulation and aged platform water will be mixed with open-marine water masses, leading to a positive trend (Immenhauser et al., 2003).

In the Tailfer section, the boundary between the *punctata* and *hassi* Zones is still subject to debate. Bultynck et al. (2000) positioned the boundary almost 45 m above the base of the Lustin Formation and Gouwy and Bultynck (2000) at 15 m above (Fig. 3, boundaries a and b between *punctata* and *hassi* Zones). In the first case (boundary a), the positive excursion is not restricted to the *punctata* Zone, but also extends into the Early *hassi* Zone, and in the second case, the positive excursion is restricted within the *punctata* Zone, to its upper boundary. This positive anomaly is recognized to be restricted within the *punctata* Zone (Pisarzowska et al., 2006; Yans et al., 2007), so the *punctata–hassi* zonal boundary is probably close to that proposed by Bultynck et al. (2000), around 30 m above the base of the Tailfer section (stratotype of the Lustin Formation).

The Frasnian of Belgium shows that vertical variations of carbon isotopes are mainly related to local structure of the basin and seawater circulation. This implies difficulties in correlating carbon isotopes excursions on a global scale. Vertical carbon isotope variations can be only related to lateral variations at the basinal scale. As showed by Panchuk et al. (2005, 2006), the presence of similar-looking carbon isotope excursions in shallow-water sea sediments might have been generated by regional sea-level variations.

8. Conclusions

This paper combines isotopic data from brachiopods, cements and matrix micrites with sedimentological and diagenetic analyses for Middle Frasnian biostromal to lagoonal shallow-water carbonates from Belgium. The succession consists of fourth-order regressive sequences (some capped by subaerial exposure), with a major regressive surface separating the Frasnian sections into a lower biostromal unit and an upper lagoonal unit. The diagenetic history consists of three main events. The first is early meteoric, which corresponds to the development of short-term periods of subaerial exposure with paleosols. The second stage is late meteoric, which is related to a major regressive surface formed during the Famennian. The late stage is burial diagenesis and corresponds to temperatures between 100 and 245 °C.

The carbon isotope values show a more negative trend with respect to fourth- and third-order sea-level changes, with the lowest values being after the main regression, at the top of fourth-order shallowing-upward sequences and within the shallowest-water microfacies and paleosols. These trends are interpreted as reflecting two main influences. The first one probably corresponds to a primary signal, with a lateral variation of the carbon isotopes in the Frasnian seawater relating to the restriction of the platform ("aging" of the platform water, Patterson and Walter, 1994). The second influence corresponds largely to early meteoric diagenesis (pedogenesis).

These data reflect the influence of sea-level and water circulation on carbon isotopes for shallow-water deposits and this influence implies that shallow-water carbonates are not necessarily good material for assessing the primary carbon isotopic values of the ocean because of the influence of long residence time ("aging") of the platform-top water and because of related lateral variations of carbon isotope signals.

Acknowledgements

This study forms part of the first author's Ph.D. dissertation at the University of Liège. This Ph.D. was carried out with the financial support of an F.R.I.A. grant from the Belgian Fond National de la Recherche Scientifique (FNRS). Anne-Christine da Silva acknowledges the F.N.R.S. (Belgium) for a position of Postdoctoral Researcher. Isotopic analyses were performed with the financial support of the French CNRS Eclipse Project (special thanks to Olivier Averbuch, University of Lille). We are especially grateful to Maurice Tucker, Jared Morrow, Michael Joachimski, Chris Holmden, Grzegorz Racki and Jindřich Hladil for their very constructive critical reading and their comments, which have helped greatly to improve this paper.

Appendix A. Oxygen and carbon isotopic data and stratigraphic position (in metres) from the different sections

Sample number	Strat. pos.	$\delta^{13}C$	$\delta^{18}O$
Tailfer section			
L11b	6	3.80	−7.68
L12	6.85	3.75	−8.08
L12b	8.15	3.16	−8.16
L13	23.7	2.95	−6.99
L28c	26.1	4.83	−6.60
L30	26.25	4.62	−6.32
L30b	26.5	4.22	−6.38
L31b	27.6	4.13	−6.17
L34	27.75	4.18	−6.00
L35	28	4.21	−6.23
L42	33.25	3.52	−6.00
L42c	34.8	3.23	−5.74
L42d	35.2	3.30	−5.88
L42f	36.25	3.14	−6.01
L42h	37.75	2.60	−5.73
L42i	38.25	3.19	−5.86
L43	38.6	3.18	−5.91
L43b	39	3.12	−5.7
L43c	39.4	2.91	−5.92
L43e	40.3	2.91	−5.92
L44	40.75	3.10	−5.92
L44c	41.5	2.85	−5.67
L44d	41.75	3.14	−5.39
L44e	42.25	2.77	−5.55
L44f	42.9	3.03	−5.95
L44h	43.6	2.44	−5.48
L47	46	2.34	−6.56
L47c	47.1	2.39	−6.7

(continued on next page)

Appendix A (*continued*)

Sample number	Strat. pos.	$\delta^{13}C$	$\delta^{18}O$
Tailfer section			
L47d	48	1.52	−6.57
L51	51	2.19	−5.81
L51b	51.7	2.53	−5.96
L51c	51.8	3.28	−5.00
L53	53.6	1.40	−6.41
L53b	54	1.71	−6.39
L56b	56.6	0.34	−6.41
L57	56.9	0.11	−6.62
L57b	57.4	0.80	−6.49
L58	58.3	−0.62	−6.50
L59b	59.2	−0.45	−6.61
L60b	60.1	−2.58	−6.94
L61	60.2	−2.78	−7.02
L61c	61	−1.94	−7.10
L62	61.1	−2.28	−7.10
L62c	62.1	−1.39	−7.29
L63b	63	−2.75	−7.08
L63c	63.5	−0.96	−7.17
L64	64.1	−1.52	−7.22
L65	64.2	−0.91	−7.06
L66b	64.9	−1.12	−7.28
L67	65.5	−1.79	−7.25
L67b	66	−0.90	−7.46
L68	66.1	−1.24	−7.43
L70	67.1	−2.14	−7.41
L70b	67.5	−0.72	−7.42
L70c	67.75	−0.15	−7.36
L70c(2)	67.75	−1.95	−7.26
L71	68.1	−2.25	−7.38
L72a	69	−7.45	−7.11
L72b	69	−1.73	−7.35
L72B	69.2	−3.21	−7.34
L73	69.6	−2.70	−7.50
L73b	69.9	−3.20	−7.38
L73c	70.1	−4.36	−7.30
L74	70.9	−2.73	−7.51
L74b	71.3	−3.08	−7.21
L76	72.5	−3.29	−7.19
L77	72.9	−6.54	−7.28
L77b	73.6	−5.07	−7.19
L78c	74.1	−0.03	−7.10
L79b	74.3	0.34	−6.93
L80b	74.4	−0.77	−6.68
L81	74.7	−2.26	−7.00
L81b	75	−1.33	−6.63
L82	75.2	−0.95	−6.72
L85a	76.4	−2.12	−6.11
L87b	77.5	−1.43	−6.54
L87c	77.7	−1.65	−6.79
L89a	78.2	−4.85	−6.62
L92	79.6	−4.35	−6.79
L93	79.7	−2.69	−6.76
L97	81.7	−0.40	−6.61
L98	81.9	−0.65	−6.79
L98b	82.2	−0.39	−6.59
L99b	82.7	−0.71	−6.81
L101	83.4	−0.14	−6.79
L102	83.6	−0.36	−5.54
L102b	84	−0.41	−5.31
L103b	85	−0.85	−6.63
L103c	85.2	−1.03	−5.63
L104b	85.6	−1.19	−6.60
L104c	85.7	−1.04	−6.40
L106	86.05	−1.32	−6.67
L106b	86.05	−1.00	−6.60
L107	86.6	−0.85	−6.56
L107b	86.95	−0.72	−6.58
L108	87	−0.47	−6.61
L108b	87.1	−1.07	−6.44
L109	87.55	−1.69	−6.55
L109b	87.7	−1.81	−6.58
L110	87.8	−1.51	−6.50
L114b	88.9	0.57	−6.55
L114d	89.2	0.71	−6.66
L115b	89.7	0.51	−6.93

Appendix A (*continued*)

Sample number	Strat. pos.	$\delta^{13}C$	$\delta^{18}O$
Tailfer section			
L116	89.9	0.73	−6.74
L117	90.3	0.71	−6.54
L117b	90.4	1.35	−6.62
L118	90.8	0.46	−6.45
L118b	91.1	0.39	−6.59
L118c	91.35	−0.24	−6.6
L119b	92	−0.59	−6.78
L119c	92.5	−1.03	−6.71
L120	92.55	−0.37	−6.73
L123	93.5	0.05	−6.7
L123c	93.8	−0.10	−6.63
L124	93.9	−0.49	−6.65
L130	96.7	−1.76	−6.48
L134b	97.8	0.08	−7.12
L137b	98.75	−0.01	−7.52
L138	98.9	−0.76	−7.51
L138c	99.7	−0.05	−7.89
L139	99.8	0.07	−8.14
L140b	100.5	0.22	−8.54
L142	101	−0.34	−8.77
L142b	101.5	0.36	−8.41
Colonster section			
C9a	5.5	1.23	−7.64
C11	8.7	2.42	−7.20
C16E	16.6	1.94	−7.10
C24M	28.7	−2.92	−7.87
C25	30.7	−5.86	−7.91
Aywaille section			
AW39	13.6	1.25	−8.50
A79	57.6	2.36	−8.22
A124	84	−2.10	−7.82
A129	87	−4.94	−7.48
A167C	111.1	0.03	−7.57
Villers section			
V10	6.9	2.99	−8.31
V47C	22.8	2.66	−7.42
V74	59.6	1.71	−8.84
V86	75	2.21	−7.19

Sample number	Section	$\delta^{13}C$	$\delta^{18}O$
Brachiopods			
C16 BR	Colonster	1.94	−7.10
A49 BR	Aywaille	2.78	−6.40
B13 BR	Barse	1.95	−4.50
Mean values		2.22	−6.00
Cement (2) non-luminescent calcite			
LIIB1	Tailfer	3.83	−5.82
LIIB2	Tailfer	3.49	−6.37
V91	Villers	1.52	−10.44
V78	Villers	2.52	−7.44
Mean values		2.76	−7.52
Cement (4) dull calcite			
V91 C4	Villers	2.42	−7.22
B13 C4	Barse	2.33	−3.92
B1C C4	Barse	1.09	−6.35
Mean values		1.95	−5.83

References

Algeo, J.T., 1996. Meteoric water/rock ratios and the significance of sequence and parasequence boundaries in the Gobbler Formation (Middle Pennsylvanian) of South-central New Mexico. In: Witzke, B.J., Ludvigson, G.A., Day, J. (Eds.), Paleozoic Sequence Stratigraphy: Views from the North American Craton: Boulder, Colorado. Geol. Soc. Am., Spec. Pap., vol. 306, pp. 359–371.

Algeo, T.J., Wilkinson, B.H., Lohman, K.C., 1992. Meteoric — burial diagenesis of Middle Pennsylvanian limestones in the Orogrande basin, New Mexico: water/rock interactions and basin geothermics. J. Sediment. Petrol. 62, 652–670.

Allan, J.R., Matthews, R.K., 1977. Carbon and oxygen isotopes as diagenetic and stratigraphic tools: surface and subsurface data, Barbados, West Indies. Geology 5, 16–20.

Allan, J.R., Matthews, R.K., 1982. Isotope signatures associated with early meteoric diagenesis. Sedimentology 29, 797–817.

Bábek, O., Prikryl, T., Hladil, J., 2007. Progressive drowning of carbonate platform in the Moravo–Silesian Basin (Czech Republic) before the Frasnian/Famennian event: facies, compositional variations and gamma-ray spectrometry. Facies 53, 293–316.
Baliński, A., Olempska, E., Racki, G. (Eds.), 2006. Biotic Aspects of the Early–Middle Frasnian Eventful Transition. Acta Palaeont. Pol., vol. 51, pp. 605–828.
Banner, J.L., Hanson, G.N., 1990. Calculation of simultaneous isotopic and trace element variations during water–rock interaction with applications to carbonate diagenesis. Geochim. Cosmochim. Acta 54, 3123–3137.
Becker, R.T., House, M.R., 1998. Proposal for an international substage subdivision of the Frasnian. SDS Newsl. 15, 17–22 http://sds.uta.edu/Newsletter15/nl15body.htm.
Boulvain, F., 1993. Sédimentologie et diagenèse des monticules micritiques frasniens "F2j" de l'Ardenne. Service Geologique de Belgique 260 P.P. 427 pp.
Boulvain, F., 2001. Facies architecture and diagenesis of Belgian Late Frasnian carbonate mounds. Sediment. Geol. 145, 269–294.
Boulvain, F., Herbosch, A., Keppens, E., 1992. Digenèse des monticules micritiques de la partie supérieure du Frasnien du Synclinorium de Dinant (Belgique, France). Comp.-R Ac. Sc. Paris 315 (II), 551–558.
Boulvain, F., Bultynck, P., Coen, M., Coen-Aubert, M., Helsen, S., Lacroix, D., Laloux, M., Casier, J.G., Dejonghe, L., Dumoulin, V., Ghysel, P., Godefroid, J., Mouravieff, N., Sartenaer, P., Tourneur, F., Vanguestaine, M., 1999. Les formations du Frasnien de la Belgique. Mem. Geol. Surv. Belg. 44 125 pp.
Brett, C.E., Baird, G.C., 1996. Middle Devonian sedimentary cycles and sequences in the northern Appalachian Basin. In: Witzke, B.J., Ludvingson, G.A., Day, J. (Eds.), Paleozoic Sequence Stratigraphy; Views from the North American Craton. Geol. Soc. Am. Spec. Pap., vol. 306, pp. 213–241.
Bultynck, P., Coen-Aubert, M., Godefroid, J., 2000. Summary of the state of correlation in the Devonian of the Ardennes (Belgium — NE France) resulting from the decisions of the SDS. In: Bultynck, P. (Ed.), Subcommission on Devonian Stratigraphy: Recognition of Devonian Series and Stage Boundaries in Geological Areas. Cour. Forsch.-Inst. Senckenberg, vol. 225, pp. 91–114.
Buonocunto, F.P., Sprovieri, M., Bellanca, A., D'Argenio, B., Ferreri, V., Neri, R., Ferruzza, G., 2002. Cyclostratigraphy and high-frequency carbon isotope fluctuations in Upper Cretaceous shallow-water carbonates, southern Italy. Sedimentology 49, 1321–1337.
Burchette, T.P., 1981. European Devonian reefs; a review of currents concepts and models. In: Toomey, D.F. (Ed.), European Fossil Reef Models. Soc. Econ. Paleont. Mineral. Spec. Publ., vol. 30, pp. 85–142.
Chen, D., Tucker, M.E., Jiang, M., Zhu, J., 2001a. Long distance correlation between tectonic controlled, isolated carbonate platforms by cyclostratigraphy and sequence stratigraphy in the Devonian of South China. Sedimentology 48, 57–78.
Chen, D., Tucker, M.E., Zhu, J., Jiang, M., 2001b. Carbonate sedimentation in a starved pull-apart basin, Middle to Late Devonian, southern Guilin, South China. Basin Res. 13, 141–168.
Chen, D., Tucker, M.E., Shen, Y., Yans, J., Préat, A., 2002. Carbon isotope excursions and sea-level change: implications for the Frasnian–Famennian biotic crisis. J. Geol. Soc. London 159, 623–626.
Chen, D., Qing, H., Li, R., 2005. The Late Devonian Frasnian–Famennian (F/F) biotic crisis: insights from $\delta^{13}C_{carb}$, $\delta^{13}C_{org}$ and $^{87}Sr/^{86}Sr$ isotopic systematics. Earth Planet. Sci. Lett. 235, 151–166.
Cloetingh, S., 1988. Intraplate stresses: a tectonic cause for third-order cycles in apparent sea level ? In: Wilgus, C.K. (Ed.), Sea Level Changes an Integrated Approach,.), Sea Level Changes: An Integrated Approach. Soc. Econ. Paleont. Mineral. Spec. Publ., vol. 42, pp. 19–29.
Copper, P., 2002. Silurian and Devonian reefs: 80 million years of global greenhouse between two ice ages. In: Kiessling, W., Fluegel, E., Golonka, J. (Eds.), Phanerozoic Reef Patterns. Soc. Econ. Paleont. Mineral. Spec. Publ., vol. 72, pp. 181–238.
da Silva, A.C., 2004. Sédimentologie de la plate-forme carbonatée frasnienne belge. Unpublished Ph.D. Thesis, Université de Liège, Liège, Belgium, 253 pp.
da Silva, A.C., Boulvain, F., 2002. Sedimentology, magnetic susceptibility and isotopes of a Middle Frasnian Carbonate platform: Tailfer section, Belgium. Facies 46, 89–102.
da Silva, A.C., Boulvain, F., 2004. From palaeosoils to carbonate mounds: facies and environments of Middle Frasnian carbonate platform in Belgium. In: Racki, G., Narkiewicz, M. (Eds.), Multidisciplinary Event Approaches to the Devonian Stratigraphic Record. Geol. Quart., vol. 48, pp. 253–266.
da Silva, A.C., Boulvain, F., 2006. Upper Devonian carbonate platform correlations and sea-level variations recorded in magnetic susceptibility. Palaeogeogr. Palaeoclimatol. Palaeoecol. 240, 373–388.
Day, J., 1996. Faunal signatures of Middle–Upper Devonian depositional sequences and sea-level fluctuations in the Iowa Basin: US Mid-Continent. In: Witzke, B.J., Ludvigson, G.A., Day, J. (Eds.), Paleozoic Sequence Stratigraphy, Views from the North American Craton. Geol. Soc. Am. Spec. Pap., vol. 306, pp. 277–300.
Donovan, D.T., Jones, E.J.W., 1979. Causes of world-wide changes in sea level. J. Geol. Soc. (Lond.) 136, 187–192.
Elrick, M., 1995. Cyclostratigraphy of Middle Devonian carbonates of the eastern Great Basin. J. Sediment. Res. B65, 61–79.
Elrick, M., 1996. Sequence stratigraphy and platform evolution of Lower–Middle Devonian carbonates, eastern Great Basin. Geol. Soc. Am., Bull. 108, 392–416.
Elrick, M., Read, J.F., 1991. Cyclic ramp-to-basin carbonate deposits, Lower Mississippian Wyoming and Montana: a combined field and computer modeling study. J. Sediment. Petrol. 61, 1194–1224.
Fielitz, W., Mansy, J., 1999. Pre- and syn-orogenic burial metamorphism in the Ardenne and neighbouring areas (Rhenohercynian zone, central European Variscides). Tectonophysics 309, 227–256.
Flügel, E., 1982. Microfacies Analysis of Limestones. Springer-Verlag, Berlin. 633 pp.
Garland, J., Tucker, M.E., Scrutton, C.T., 1996. Microfacies analysis and metre-scale cyclicity in the Givetian back-reef sediments of south-east Devon. Proc. Ussher Soc. 40, 31–36.
Gersl, M., Hladil, J., 2004. Gamma-ray and magnetic susceptibility correlation across a Frasnian carbonate platform and the search for "*punctata*" equivalents in stromatoporoid-coral limestone facies of Moravia. In: Racki, G., Narkiewicz, M. (Eds.), Multidisciplinary Event Approaches to the Devonian Stratigraphic Record. Geol. Quart., vol. 48, pp. 283–292.
Ginsburg, R.N., 1971. Landward movement of carbonate mud: new model for regressive cycles in carbonates (Abstr.). Am. Assoc. Petrol. Geol. Bull. 55, 340.
Goddéris, Y., Joachimski, M., 2004. Global change in the Late Devonian: modelling the Frasnian–Famennian short-term carbon isotope excursions. Palaeogeogr. Palaeoclimatol. Palaeoecol. 202, 309–329.
Goldhammer, R.K., Lehmann, P.J., Dunn, P.A., 1993. The origin of high-frequency platform carbonate cycles and third-order sequences (Lower Ordovician El Paso GP, West Texas): constraints from outcrop data and stratigraphic modelling. J. Sediment. Petrol. 63, 318–359.
Goldstein, R.H., 1991. Stable isotope signatures associated with palaeosoils, Pennsylvanian Holder Formation, New Mexico. Sedimentology 38, 67–77.
Gouwy, S., Bultynck, P., 2000. Graphic correlation of Frasnian sections (Upper Devonian) in the Ardennes, Belgium. Bull. Inst. Roy. Sc. Nat. Belgique 70, 25–52.
Hardie, L.A., 1977. Sedimentation on the Modern Carbonate Tidal Flats of Northwest Andros Island, Bahamas. John Hopkins Univer. Press, Baltimore.
Helsen, S., 1992. Conodont colour alteration maps for Paleozoic strata in Belgium, Northern France and Westernmost Germany — preliminary results. Ann. Soc. Géol. Belgique 115 (1), 135–143.
Helsen, S., 1995. Burial history of Paleozoic strata in Belgium as revealed by conodont colour alteration data and thickness distributions. Geol. Rundsch. 84, 738–747.
Hladikova, J., Hladil, J., Zuskova, J., 1997. Discrimination between facies and global controls in isotope composition of carbonates: carbon and oxygen isotopes at the Devonian reef margin in Moravia (HV-105 Krtiny borehole). J. Czech Geol. Soc. 42, 1–16.
Hladil, J., 2002. Geophysical records of dispersed weathering products on the Frasnian carbonate platform and early Famennian ramps in Moravia, Czech Republic: proxies for eustasy and palaeoclimate. In: Racki, G., House, M.R. (Eds.), Late Devonian Biotic Crisis: Ecological, Depositional and Geochemical Records. Palaeogeogr. Palaeoclimatol. Palaeoecol., vol. 181, pp. 213–250.
Hladil, J., Gersl, M., Strnad, L., Frana, J., Langrova, A., Spisiak, J., 2005. Stratigraphic variations of complex impurities in platform limestones and possible significance of atmospheric dust: a study emphasis on gamma-ray spectrometry and magnetic susceptibility outcrop logging (Eifelian–Frasnian, Moravia, Czech Republic). Int. J. Earth Sc. 95, 703–723.
Holmden, C., Creaser, R.A., Muehlbachs, K., Leslie, S.A., Bergeström, S.M., 1998. Isotopic evidence for geochemical decoupling between ancient epeiric seas and bordering oceans: implications for secular curves. Geology 26, 567–570.
Holmden, C., Braun, W.K., Patterson, W.P., Eglington, B.M., Prokopiuk, T.C., Whittaker, S., 2006. Carbon isotope chemostratigraphy of Frasnian Sequences in Western Canada. Saskatchewan Geol. Surv. Summ. Investig. 1, 1–6.
House, M.R., 2002. Strength, timing, setting and cause of mid-Paleozoic extinctions. In: Racki, G., House, M.R. (Eds.), Late Devonian Biotic Crisis: Ecological, Depositional and Geochemical Records. Palaeogeogr. Palaeoclimatol. Palaeoecol., vol. 181, pp. 5–25.
Hurley, N.F., Lohmann, K.C., 1989. Diagenesis of Devonian reefal carbonates in the Oscar Range, Canning Basin, Western Australia. J. Sediment. Petrol. 59, 127–146.
Immenhauser, A., Kenter, J.A.M., Ganssen, G., Bahamonde, J.R., Van Vliet, A., Saher, M.H., 2002. Origin and significance of isotope shifts in Pennsylvanian carbonates (Asturias, NW Spain). J. Sediment. Petrol. 72, 82–94.
Immenhauser, A., Della Porta, G., Kenter, J.A.M., Bahamonde, J.R.A., 2003. An alternative model for positive shifts in shallow-marine carbonate $\delta^{13}C$ and $\delta^{18}O$. Sedimentology 50, 953–959.
James, N.P., 1983. Reef environment in carbonate depositional environments. In: Scholle, P.A., Bedout, D.G., Moore, C.H. (Eds.), Carbonate Depositional Environment. Am. Assoc. Petrol. Geol. Mem., vol. 33, pp. 345–440.
James, N.P., 1984. Shallowing-upward sequences in carbonates, In: Walker, R.G. (Ed.), Facies Models, 2nd edition. . Geoscience Canada, Reprint series, vol. 1, pp. 213–228.
Joachimski, M.M., 1994. Subaerial exposure and deposition of shallowing-upward sequences: evidence from stable isotopes of Purbeckian peritidal carbonates (basal Cretaceous), Swiss and French Jura Mountains. Sedimentology 41, 805–824.
Joachimski, M.M., 1997. Comparison of organic and inorganic carbon isotope patterns across the Frasnian–Famennian boundary. In: Geldsetzer, H.H.J., Joachimski, M.M. (Eds.), Geochemical Event Markers in the Phanerozoic. Palaeogeogr. Palaeoclimatol. Palaeoecol., vol. 132, pp. 133–145.
Joachimski, M.M., Ostertag-Henning, C., Pancost, R.D., Pancost, R.D., Strauss, H., Freeman, K.H., Littke, R., Sinninghe Damsté, J., Racki, G., 2001. Water column anoxia, enhanced productivity and concomitant changes in delta^{13}C and delta^{34}S across the Frasnian–Famennian boundary (Kowala — Holy Cross Mountains/ Poland). Chem. Geol. 175, 109–131.
Joachimski, M.M., Pancost, R.D., Freeman, K.H., Buggisch, W., 2002. Carbon isotope geochemistry of the Frasnian–Famennian transition. In: Racki, G., House, M.R. (Eds.), Late Devonian Biotic Crisis: Ecological, Depositional and Geochemical Records. Palaeogeogr. Palaeoclimatol. Palaeoecol., vol. 181, pp. 91–109.
Joachimski, M.M., Van Geldern, R., Breisig, S., Buggisch, W., Day, J., 2004. Oxygen isotope evolution of biogenic calcite and apatite during the Middle and Late Devonian. Int. J. Earth Sc. 93, 542–553.
Johnson, J.G., Klapper, G., Sandberg, C.A., 1985. Devonian eustatic fluctuations in Euramerica. Geol. Soc. Am. Bull. 96, 567–587.
Kaufmann, B., 2006. Calibrating the Devonian Time-Scale: a synthesis of U–Pb ID-TIMS ages and conodont stratigraphy. Earth-Sci. Rev. 76, 175–190.
Keith, M.L., Parker, R.H., 1965. Local variations of 13-C and 18-O content of mollusc shells and relatively minor temperature effect in marginal marine environment. Mar. Geol. 3, 115–129.

Kershaw, S., 1998. The applications of stromatoporoid palaeobiology in palaeoenvironmental analysis. Palaeontology 41, 509–544.
Kiessling, W., Flügel, E., Golonka, J., 1999. Paleoreef maps: evaluation of a comprehensive database on Phanerozoic reefs. Am. Assoc. Petrol. Geol., Bull. 83, 1552–1587.
Lloyd, M.R., 1964. Variations in the oxygen and the carbon isotope ratios of Florida Bay molluscs and their environmental significance. J. Geol. 72, 84–111.
Lohmann, K.C., 1988. Geochemical patterns of meteoric diagenetic systems and their application to studies of paleokarst. In: James, N.P., Choquette, P.W. (Eds.), Paleokarst. Springer Verlag, pp. 58–80.
Machel, H.G., Hunter, I.G., 1994. Facies model for Middle to Late Devonian shallow-marine carbonates, with comparisons to modern reefs: a guide for facies analysis. Facies 30, 155–176.
MacNeil, A.J., Jones, B., 2006. Sequence stratigraphy of a Late Devonian ramp-situated reef system in the Western Canada Sedimentary Basin: dynamic responses to sea-level change and regressive reef development. Sedimentology 53, 321–359.
Mamet, B.L., 1970. Sur les *Umbellaceae*. Can. J. Earth Sc. 7, 1164–1171.
Marquillas, R., Sabino, I., Nobrega Sial, A., Papa, C.D., Ferreira, V., Matthews, S., 2007. Carbon and oxygen isotopes of Maastrichtian–Danian shallow marine carbonates: Yacoraite Formation, northwestern Argentina. J. South Am. Earth Sc. 23, 304–320.
May, A., 1992. Palaeoecology of Upper Eifelian and Lower Givetian coral limestones in the Northwestern Sauerland (Devonian; Rhenish Massif). Facies 26, 103–116.
McLean, D.J., Mountjoy, E.W., 1994. Allocyclic control on Late Devonian buildup development, Southern Canadian Rocky Mountains. J. Sediment. Res. B64, 326–340.
Méndez-Bedia, I., Soto, F.M., Fernández-Martínez, E., 1994. Devonian reef types in the Cantabrian Mountains (NW Spain) and their faunal composition. Cour. Forsch.-Inst. Senckenberg 172, 161–183.
Meyers, W.J., Lohmann, K.C., 1985. Isotope geochemistry of regionally extensive calcite cement zones and marine components in Mississippian limestones, New Mexico. In: Schneidermann, N., Harris, P.M. (Eds.), Carbonate Cements. Soc. Econ. Paleont. Mineral. Spec. Publ., vol. 36, pp. 223–239.
Mörner, N.A., 1994. Internal response to orbital forcing and external cyclic sedimentary sequences. In: De Boer, P.L., Smith, D.G. (Eds.), Orbital Forcing and Cyclic Sequences. Int. Ass. Sed. Spec. Publ., vol. 19, pp. 25–33.
Osleger, D., 1991. Subtidal carbonate cycles: implications for allocyclic vs. autocyclic controls. Geology 19, 917–920.
Panchuk, K.M., Holmden, C., Kump, L.R., 2005. Sensitivity of the epeiric sea carbon isotope record to local-scale carbon cycle processes: tales from the Mohawkian Sea. Palaeogeogr, Palaeoclimatol. Palaeoecol. 228, 320–337.
Panchuk, K.M., Holmden, C., Leslie, S.A., 2006. Local controls on carbon cycling in the Ordovician midcontinent region of north America, with implications for carbon isotope secular curves. J. Sediment. Geol. 76, 200–211.
Patterson, W.P., Walter, L.M., 1994. Depletion of ^{13}C in sea water SCO_2 on modern carbonate platforms: significance for the carbon isotopic record of carbonates. Geology 22, 885–888.
Pisarzowska, A., Sobstel, M., Racki, G., 2006. Conodont-based event stratigraphy of the Early–Middle Frasnian transition on the South Polish carbonate shelf. In: Balinski, A., Olempska, E., Racki, G. (Eds.), Biotic Aspects of the Early–Middle Frasnian eventful transition.Eventful Transition. Acta Palaeont. Pol. 51, 606–608.
Playford, P.E., 2002. Palaeokarst, pseudokarst and sequence stratigraphy in Devonian reef complexes of the Canning Basin, Western Australia. In: Keep, M., Moss, S.J. (Eds.), The Sedimentary Basins of Western Australia. Proc. Petrol. Explor. Soc. Australia Symposium, vol. 3, pp. 763–793.
Pohler, S.M.L., 1998. Devonian carbonate buildup facies in an intra-oceanic island arc (Tamworth Belt, New South Wales, Australia). Facies 39, 1–34.
Racki, G., Pietchota, A., Bond, D., Wignall, B., 2004. Geochemical and ecological aspects of lower Frasnian pyrite-ammonoid levels at Kostomloty (Holy Cross Mountains, Poland). In: Racki, G., Narkiewicz, M. (Eds.), Multidisciplinary Event Approaches to the Devonian Stratigraphic Record. Geol. Quart., vol. 48, pp. 267–282.
Sobstel, M., Makowska-Haftka, M., Racki, G., 2006. Conodont ecology in the Early–Middle Frasnian transition on the South Polish carbonate shelf. In: Balinski, A., Olempska, E., Racki, G. (Eds.), Biotic Aspects of the Early–Middle Frasnian Eventful Transition. Eventful Transition. Acta Palaeont. Pol., vol. 51, pp. 719–746.
Stephens, N.P., Sumner, D.Y., 2003. Late Devonian carbon isotope stratigraphy and sea-level fluctuations, Canning basin, Western Australia. Palaeogeogr. Palaeoclimatol. Palaeoecol. 191, 203–219.
Strasser, A., 1988. Shallowing-upward sequences in Purbeckian peritidal carbonates (lowermost Cretaceous, Swiss and French Jura Mountains). Sedimentology 35, 369–383.
Streel, M., Caputo, M.V., Loboziak, S., Melo, J.H.G., 2000. Late Frasnian–Famennian climates based on palynomorph analyses and the question of the Late Devonian glaciations. Earth-Sc. Rev. 52, 121–173.
Tucker, M.E., Wright, V.P., 1990. Carbonate Sedimentology. Blackwell Science, Oxford.
Vail, P.R., Mitchum Jr., R.M., Thompson, S., 1977. Seismic stratigraphy and global changes of sea level, part 4: global cycles of relative changes of sea level. In: Payton, C.E. (Ed.), Seismic Stratigraphy — Applications to Hydrocarbon Exploration. Am. Assoc. Petrol. Geol. Mem., vol, 26, pp. 83–97.
Veizer, J., Fritz, P., Jones, B., 1986. Geochemistry of brachiopods, oxygen and carbon isotopic records of Paleozoic oceans. Geochim. Cosmochim. Acta 50, 1679–1696.
Veizer, J., Ala, D., Azmy, K., Bruckschen, P., Buhl, D., Bruhn, F., Carden, G.A.F., Diener, A., Ebneth, S., Goddéris, Y., Jasper, T., Korte, C., Pawellek, F., Podlaha, O.G., Strauss, H., 1999. $^{87}Sr/^{86}Sr$, $d^{13}C$ and $d^{18}O$ evolution of Phanerozoic seawater. In: Allègre, C.J., Arndt, N.T., Bickle, M.J., et al. (Eds.), Earth System Evolution: Geochemical Perspective. Chem. Geol., vol. 161, pp. 59–88.
Wachter, E., Hayes, J.M., 1985. Exchange of oxygen isotopes in carbon dioxide–phosphoric acid systems. Chem. Geol. 52, 365–374.
Whalen, M.T., Day, J.E., 2005. Magnetic susceptibility, biostratigraphy, and sequence stratigraphy: insights into Devonian carbonate platform development and basin infilling, western Alberta. Am. Assoc. Petrol. Geol. Annual Convention Abstr. vol. 14, A151.
Whalen, M.T., Eberli, G.P., Van Buchem, F.S.P., Mountjoy, E.W., 2000. Facies models and architecture of Upper Devonian carbonate platforms (Miette and Ancient wall), Alberta, Canada. In: Homewood, P.W., Eberli, G.P. (Eds.), Genetic stratigrapExploration and the production scales.Production Scales. Case studiesStudies from the Pennsylvanian of the Paradox basinBasin and the Upper Devonian of Alberta. Bull C. Rech. Expl.-Prod. Elf-Aquitaine, Mém., vol. 24, pp. 139–178.
Wilson, J.L., 1975. Carbonate Facies in Geologic History. Springer-Verlag, Berlin, Heidelberg, New York.
Wood, R., 1998. Reef Evolution. Oxford Univ. Press, Oxford.
Wood, R., 2000. Palaeoecology of a late Devonian back reef: Canning Basin, Western Australia. Palaeontology 43, 671–703.
Wright, V.P., 1994. Paleosols in shallow marine carbonate sequences. Earth-Sc. Rev. 35, 367–395.
Yans, J., Corfield, R.M., Racki, G., Préat, A., 2007. Evidence for perturbation of the carbon cycle in the Middle Frasnian *punctata* conodont Zone. Geol. Mag. 144, 263–270.
Zhuravlev, A.V., Sokiran, S., Evdokimova, I.O., Dorofeeva, L.A., Rusetskaya, G.A., Malkowski, K., 2006. Faunal and facies changes at the Early–Middle Frasnian boundary in the north-Western East European platform. In: Balinski, A., Olempska, E., Racki, G. (Eds.), Biotic Aspects of the Early–Middle Frasnian Eventful Transition. Eventful Transition. Acta Palaeontol. Pol., vol. 51, pp. 747–758.